HAL
archives-ouvertes.fr

Residual-based a posteriori error estimation for contact problems approximated by Nitsche's method

Franz Chouly, Mathieu Fabre, Patrick Hild, Jérôme Pousin, Yves Renard

▶ To cite this version:

Franz Chouly, Mathieu Fabre, Patrick Hild, Jérôme Pousin, Yves Renard. Residual-based a posteriori error estimation for contact problems approximated by Nitsche's method. 2015. <hal-01143168>

HAL Id: hal-01143168
https://hal.archives-ouvertes.fr/hal-01143168

Submitted on 16 Apr 2015

Residual-based *a posteriori* error estimation for contact problems approximated by Nitsche's method

Franz Chouly [*]   Mathieu Fabre [†]   Patrick Hild [‡]   Jérôme Pousin [§]

Yves Renard [¶]

April 14, 2015

Abstract

We introduce a residual-based *a posteriori* error estimator for contact problems in two and three dimensional linear elasticity, discretized with linear and quadratic finite elements and Nitsche's method. Efficiency and reliability of the estimator are proved under a saturation assumption. Numerical experiments illustrate the theoretical properties and the good performance of the estimator.

Key words: unilateral contact, finite elements, Nitsche's method, *a posteriori* error estimates, residuals.
AMS Subject Classification: 65N12, 65N30, 74M15.

1   Introduction

The computations of contact problems between deformable bodies are usually obtained with the finite element method [39, 51]. An important aspect for the user is to quantify the quality of the simulations by evaluating the discretization errors coming from the finite element approximation. This quantification requires the definition of *a posteriori* error estimators which can be of different types (residual based, equilibrated fluxes, smoothing of the stress fields ...). The main aim of the estimators is to furnish some information on the local error in order to adapt or refine the mesh and to reduce the computational costs.

Among the finite element discretizations for contact problems, a recent effort was devoted to Nitsche's method which can be seen as a consistent penalty formulation with only one primal unknown (like the penalty or the variational inequality formulation): the displacement field. In contrast to Nitsche's method, the Lagrange (stabilized or standard) methods admit the contact

[*]Laboratoire de Mathématiques de Besançon - UMR CNRS 6623, Université de Franche Comté, 16 route de Gray, 25030 Besançon Cedex, France. email: `franz.chouly@univ-fcomte.fr`

[†]Université de Lyon, CNRS, INSA-Lyon, ICJ UMR5208, F-69621, Villeurbanne, France. email: `mathieu.fabre@insa-lyon.fr`

[‡]Institut de Mathématiques de Toulouse - UMR CNRS 5219, Université Paul Sabatier, 118 route de Narbonne, 31062 Toulouse Cedex 9, France. email: `patrick.hild@math.univ-toulouse.fr`

[§]Université de Lyon, CNRS, INSA-Lyon, ICJ UMR5208, F-69621, Villeurbanne, France. email: `Jerome.Pousin@insa-lyon.fr`

[¶]Université de Lyon, CNRS, INSA-Lyon, ICJ UMR5208, LaMCoS UMR5259, F-69621, Villeurbanne, France. email: `Yves.Renard@insa-lyon.fr`

1

pressure as a supplementary unknown. Nitsche's method was introduced for the frictionless unilateral contact problem in a simple (symmetric) form in [15] then generalized and numerically investigated in [16]. In the latter references the theoretical results deal with well-posedness of the discrete problems and a priori error estimates in two and three space dimensions with linear and quadratic finite elements. A generalization to frictional contact problems is carried out in [14] (numerical analysis for Tresca friction) and [44] (numerical study for Coulomb friction). To our knowledge the *a posteriori* quantification of the discretization errors committed by the Nitsche finite element approximation has not been considered for unilateral contact problems up to now.

Nevertheless there are several studies concerning *a posteriori error* analyses for frictionless or frictional contact problems in [13, 24, 40, 52] (residual approach using a penalization of the contact condition or the normal compliance law), in [18, 19, 42, 48, 50] (equilibrated residual method), in [21, 43] (residual approach for BEM-discretizations), in [9, 46] (error technique measure developed in [6]). Moreover a residual type estimator for the Signorini problem in its common formulation (variational inequality or mixed method) can be found in [30, 31, 45] and in the recent work [38].

Finally we mention that only few works are devoted to *a posteriori* error estimates for Nitsche's method, and all concern linear boundary / interface conditions. For interface conditions and elliptic problems, Hansbo and Hansbo [26] introduce a residual type estimator for a Nitsche's unfitted treatment of the interface condition. They prove an upper bound on a linear functional of the error, in the spirit of Becker and Rannacher [7]. Note as well an early work of Becker [4] in the context of optimal control for Navier-Stokes equations, with a Nitsche treatment of Dirichlet boundary condition and an *a posteriori* error estimate for the functional to minimize. Residual error estimates are introduced as well by Becker, Hansbo and Stenberg in [5] for a Nitsche-based domain decomposition with non-matching meshes. Upper bounds both in H^1 and L^2-norms are established, with help of a saturation assumption (as in [49]) for the H^1-norm. In the context of composite grids two variants of residual-based error estimates are proposed by Hansbo, Hansbo and Larson in [27]. Upper bounds in H^1-norm without any saturation assumption are proposed for both of them. Later on Juntunen and Stenberg provide in [32] a residual-based error estimator for the stabilized Bassi-Rebay discontinuous Galerkin method, that relies on Nitsche's treatment of continuity. Upper and lower bounds are proven for this method. The same authors in [33] introduce a Nitsche's method for a general boundary condition, and an associated residual error estimator. They prove an upper bound in H^1-norm under a saturation assumption (as in [10]), and they establish a lower bound too. Finally let us mention two recent papers on the Brinkman problem by Juntunen, Könnö and Stenberg [34, 37].

The paper is outlined as follows: in Section 2 the Nitsche's finite element discretization for contact problems in linear elasticity is described and the results dealing with well-posedness are recalled from [16]. In Section 3 a residual *a posteriori* error estimator is introduced, and we prove its reliability and efficiency. In Section 4 numerical experiments in 2D and 3D illustrate the theoretical results and allow to assess the quality of the estimator, for different values of the numerical parameters.

Let us introduce some useful notations. In what follows, bold letters like $\mathbf{u}, \mathbf{v}$, indicate vector or tensor valued quantities, while the capital ones (e.g., $\mathbf{V}, \mathbf{K} \dots$) represent functional sets involving vector fields. As usual, we denote by $(H^s(.))^d$, $s \in \mathbb{R}, d = 1, 2, 3$, the Sobolev spaces in one, two or three space dimensions (see [1]) with the convention $H^0 = L^2$. The usual norm (resp. semi-norm) of $(H^s(D))^d$ is denoted by $\| \cdot \|_{s,D}$ (resp. $| \cdot |_{s,D}$) and we keep the same notation for any $d = 1, 2, 3$. In the sequel the symbol $| \cdot |$ will either denote the Euclidean norm in $\mathbb{R}^d$, or the measure of a domain in $\mathbb{R}^d$. The letter C stands for a generic constant, independent of the discretization parameters.

For two scalar quantities a and b, the notation $a \lesssim b$ means there exists a constant C, independent of the mesh size parameters and of the Nitsche parameter γ_0 (see Section 2.2), such that $a \leq Cb$. Moreover, $a \sim b$ means that $a \lesssim b$ and $b \lesssim a$.

2 Setting

2.1 The unilateral contact problem

We consider an elastic body whose reference configuration is represented by the domain Ω in $\mathbb{R}^d$ with $d = 2$ or $d = 3$. Small strain assumptions are made, as well as plane strain when $d = 2$. The boundary $\partial\Omega$ of Ω is polygonal or polyhedral and we suppose that $\partial\Omega$ consists in three nonoverlapping parts Γ_D, Γ_N and the (candidate) contact boundary Γ_C, with $\mathrm{meas}(\Gamma_D) > 0$ and $\mathrm{meas}(\Gamma_C) > 0$. The (candidate) contact boundary is supposed to be a straight line segment when $d = 2$ or a polygon when $d = 3$ to simplify. The unit outward normal vector on $\partial\Omega$ is denoted $\mathbf{n}$. In its initial stage, the body is in contact on Γ_C with a rigid foundation (the extension to two elastic bodies in contact can be easily made, at least for small strain models) and we suppose that the unknown final contact zone after deformation will be included into Γ_C. The body is clamped on Γ_D for the sake of simplicity. It is subjected to volume forces $\mathbf{f} \in (L^2(\Omega))^d$ and to surface loads $\mathbf{g} \in (L^2(\Gamma_N))^d$.

The unilateral contact problem in linear elasticity consists in finding the displacement field $\mathbf{u} : \Omega \to \mathbb{R}^d$ verifying the equations and conditions (1)–(2):

$$
\begin{aligned}
\mathbf{div}\,\boldsymbol{\sigma}(\mathbf{u}) + \mathbf{f} &= \mathbf{0} & &\text{in } \Omega, \\
\boldsymbol{\sigma}(\mathbf{u}) &= \mathbf{A}\,\boldsymbol{\varepsilon}(\mathbf{u}) & &\text{in } \Omega, \\
\mathbf{u} &= \mathbf{0} & &\text{on } \Gamma_D, \\
\boldsymbol{\sigma}(\mathbf{u})\mathbf{n} &= \mathbf{g} & &\text{on } \Gamma_N,
\end{aligned}
\tag{1}
$$

where $\boldsymbol{\sigma} = (\sigma_{ij})$, $1 \leq i, j \leq d$, stands for the stress tensor field and $\mathbf{div}$ denotes the divergence operator of tensor valued functions. The notation $\boldsymbol{\varepsilon}(\mathbf{v}) = (\boldsymbol{\nabla}\mathbf{v} + \boldsymbol{\nabla}\mathbf{v}^T)/2$ represents the linearized strain tensor field and $\mathbf{A}$ is the fourth order symmetric elasticity tensor having the usual uniform ellipticity and boundedness property. For any displacement field $\mathbf{v}$ and for any density of surface forces $\boldsymbol{\sigma}(\mathbf{v})\mathbf{n}$ defined on $\partial\Omega$ we adopt the following notation

$$
\mathbf{v} = v_n\mathbf{n} + \mathbf{v_t} \quad \text{and} \quad \boldsymbol{\sigma}(\mathbf{v})\mathbf{n} = \sigma_n(\mathbf{v})\mathbf{n} + \boldsymbol{\sigma_t}(\mathbf{v}),
$$

where $\mathbf{v_t}$ (resp. $\boldsymbol{\sigma_t}(\mathbf{v})$) are the tangential components of $\mathbf{v}$ (resp. $\boldsymbol{\sigma}(\mathbf{v})\mathbf{n}$). The conditions describing unilateral contact without friction on Γ_C are:

$$
\begin{aligned}
u_n &\leq 0, & &(i) \\
\sigma_n(\mathbf{u}) &\leq 0, & &(ii) \\
\sigma_n(\mathbf{u})\,u_n &= 0, & &(iii) \\
\boldsymbol{\sigma_t}(\mathbf{u}) &= 0. & &(iv)
\end{aligned}
\tag{2}
$$

We introduce the Hilbert space $\mathbf{V}$ and the convex cone $\mathbf{K}$ of admissible displacements which satisfy the noninterpenetration on the contact zone Γ_C:

$$
\mathbf{V} := \left\{ \mathbf{v} \in (H^1(\Omega))^d \ : \mathbf{v} = \mathbf{0} \text{ on } \Gamma_D \right\}, \quad \mathbf{K} := \left\{ \mathbf{v} \in \mathbf{V} \ : \ v_n = \mathbf{v}\cdot\mathbf{n} \leq 0 \text{ on } \Gamma_C \right\}.
$$

3

We define as well

$$a(\mathbf{u}, \mathbf{v}) := \int_\Omega \boldsymbol{\sigma}(\mathbf{u}) : \boldsymbol{\varepsilon}(\mathbf{v}) \, d\Omega, \qquad L(\mathbf{v}) := \int_\Omega \mathbf{f} \cdot \mathbf{v} \, d\Omega + \int_{\Gamma_N} \mathbf{g} \cdot \mathbf{v} \, d\Gamma,$$

for any $\mathbf{u}$ and $\mathbf{v}$ in $\mathbf{V}$. From the previous assumptions, we deduce that $a(\cdot, \cdot)$ is bilinear, symmetric, $\mathbf{V}$-elliptic and continuous on $\mathbf{V} \times \mathbf{V}$. Likewise we observe that $L(\cdot)$ is a continuous linear form on $\mathbf{V}$. The weak formulation of Problem (1)-(2), as a variational inequality (see [25, 28, 35]), reads as:

$$\begin{cases} \text{Find } \mathbf{u} \in \mathbf{K} \text{ such that:} \\ a(\mathbf{u}, \mathbf{v} - \mathbf{u}) \geq L(\mathbf{v} - \mathbf{u}), \qquad \forall \mathbf{v} \in \mathbf{K}. \end{cases} \tag{3}$$

Stampacchia's Theorem ensures that Problem (3) admits a unique solution.

2.2 Finite element setting and Nitsche-based method

To approximate problem (3) we fix a family of meshes $(T_h)_{h>0}$, regular in Ciarlet's sense (see [17]), made of closed elements and assumed to be subordinated to the decomposition of the boundary $\partial\Omega$ into Γ_D, Γ_N and Γ_C. For $K \in T_h$ we recall that h_K is the diameter of K and $h := \max_{K \in T_h} h_K$. The regularity of the mesh implies notably that for any edge (or face when $d = 3$) E of K one has $h_E := |E| \sim h_K$.

Let us define E_h as the set of edges (or faces when $d = 3$) of the triangulation and define $E_h^{int} = \{E \in E_h : E \subset \Omega\}$ as the set of interior edges/faces of T_h (the edges/faces are supposed to be relatively open). We denote by $E_h^N = \{E \in E_h : E \subset \Gamma_N\}$ the set of boundary edges/faces that correspond to Neumann conditions, and similarly $E_h^C = \{E \in E_h : E \subset \Gamma_C\}$ is the set of boundary edges/faces included into the contact boundary.

For an element K, we will denote by E_K the set of edges/faces of K and according to the above notation, we set $E_K^{int} = E_K \cap E_h^{int}$, $E_K^N = E_K \cap E_h^N$, $E_K^C = E_K \cap E_h^C$. For an edge/face E of an element K, introduce $\boldsymbol{\nu}_{K,E}$ the unit outward normal vector to K along E. Furthermore, for each edge/face E, we fix one of the two normal vectors and denote it by $\boldsymbol{\nu}_E$. The jump of some vector valued function $\boldsymbol{v}$ across an edge/face $E \in E_h^{int}$ at a point $\boldsymbol{y} \in E$ is defined as

$$\llbracket \boldsymbol{v} \rrbracket_E (\boldsymbol{y}) = \lim_{\alpha \to 0^+} \boldsymbol{v}(\boldsymbol{y} + \alpha \boldsymbol{\nu}_E) - \boldsymbol{v}(\boldsymbol{y} - \alpha \boldsymbol{\nu}_E).$$

Note that the sign of $\llbracket \boldsymbol{v} \rrbracket_E$ depends on the orientation of $\boldsymbol{\nu}_E$. Finally we will need local subdomains (also called patches). As usual, let ω_K be the union of all elements having a nonempty intersection with K. Similarly for a node $\boldsymbol{x}$ and an edge/face E, let $\omega_x = \cup_{K:x \in K} K$ and $\omega_E = \cup_{x \in \overline{E}} \omega_x$.

The chosen finite element space $\mathbf{V}^h \subset \mathbf{V}$ involves standard Lagrange finite elements of degree k with $k = 1$ or $k = 2$ (see [11, 17, 22]) *i.e.*:

$$\mathbf{V}^h := \left\{ \mathbf{v}^h \in (\mathscr{C}^0(\overline{\Omega}))^d : \mathbf{v}^h|_K \in (P_k(K))^d, \forall K \in T_h, \mathbf{v}^h = \mathbf{0} \text{ on } \Gamma_D \right\}.$$

Let us introduce the notation $[\cdot]_+$ for the positive part of a scalar quantity $a \in \mathbb{R}$: $[a]_+ = a$ if $a > 0$ and $[a]_+ = 0$ otherwise. The monotonicity property below holds:

$$([a]_+ - [b]_+)(a - b) \geq ([a]_+ - [b]_+)^2 \geq 0. \tag{4}$$

Note that the condition (4) can be straightforwardly extended to real valued functions.

Let γ be a positive piecewise constant function on the contact interface Γ_C which satisfies

$$\gamma\big|_{K \cap \Gamma_C} = \gamma_0 h_K,$$

for every K that has a non-empty intersection of dimension $d-1$ with Γ_C, and where γ_0 is a positive given constant which we call the "Nitsche parameter". Note that the value of γ on element intersections has no influence.

We introduce the discrete linear operator

$$P_\gamma : \begin{array}{ccc} \mathbf{V}^h & \to & L^2(\Gamma_C) \\ \mathbf{v}^h & \mapsto & v_n^h - \gamma\, \sigma_n(\mathbf{v}^h) \end{array},$$

and the bilinear form where $\theta \in \mathbb{R}$ is a fixed parameter:

$$A_{\theta\gamma}(\mathbf{u}^h, \mathbf{v}^h) := a(\mathbf{u}^h, \mathbf{v}^h) - \int_{\Gamma_C} \theta\gamma\, \sigma_n(\mathbf{u}^h)\sigma_n(\mathbf{v}^h)\, d\Gamma.$$

Our Nitsche-based method then reads:

$$\begin{cases} \text{Find } \mathbf{u}^h \in \mathbf{V}^h \text{ such that:} \\ A_{\theta\gamma}(\mathbf{u}^h, \mathbf{v}^h) + \displaystyle\int_{\Gamma_C} \frac{1}{\gamma}\, [P_\gamma(\mathbf{u}^h)]_+ P_{\theta\gamma}(\mathbf{v}^h)\, d\Gamma = L(\mathbf{v}^h), \quad \forall\, \mathbf{v}^h \in \mathbf{V}^h. \end{cases} \tag{5}$$

We consider the quasi-interpolation (regularization) operator introduced in *e.g.* [8, formula (4.11)] and its straightforward extension to the vectorial case, that we denote $R^h : \mathbf{V} \to \mathbf{V}^h$. This operator has the following approximation and stability properties:

Lemma 2.1. *For any $\boldsymbol{v} \in \mathbf{V} \cap (H^l(\Omega))^d$, $1 \le l \le k+1$, the following estimates hold*

$$\|\boldsymbol{v} - R^h \boldsymbol{v}\|_{0,K} \ \lesssim \ h_K^l |\boldsymbol{v}|_{l,\omega_K}, \quad \forall K \in T_h, \tag{6}$$

$$\|\boldsymbol{v} - R^h \boldsymbol{v}\|_{0,E} \ \lesssim \ h_E^{l-1/2} |\boldsymbol{v}|_{l,\omega_E}, \quad \forall E \in E_h. \tag{7}$$

Moreover R^h is stable in the H^1-norm, i.e.

$$\|R^h \boldsymbol{v}\|_{1,\Omega} \lesssim \|\boldsymbol{v}\|_{1,\Omega}, \quad \forall \boldsymbol{v} \in \mathbf{V}. \tag{8}$$

Proof. Estimates (6) and (7) are provided in [8, Theorem 4.8, Remark 8]. The stability of R^h in H^1-norm is proven in [8, Theorem 4.4] (in all cases, it suffices to apply the results of [8] component-wise). $\qquad\square$

We next define a convenient mesh dependent norm which is in fact a weighted $L^2(\Gamma_C)$-norm (since $\gamma/\gamma_0 = h_K$).

Definition 2.2. *For any $v \in L^2(\Gamma_C)$, we set*

$$\|v\|_{-1/2,h,\Gamma_C} := \left\| \left(\frac{\gamma}{\gamma_0}\right)^{\frac{1}{2}} v \right\|_{0,\Gamma_C}.$$

We end this subsection with a discrete trace inequality, that will be useful for the analysis (for the proof, see, e.g., [16]):

Lemma 2.3. *For any $\mathbf{v}^h \in \mathbf{V}^h$, we have*

$$\|\sigma_n(\mathbf{v}^h)\|_{-1/2,h,\Gamma_C} \lesssim \|\mathbf{v}^h\|_{1,\Omega}. \tag{9}$$

2.3 Consistency and well-posedness of the Nitsche-based method

We recall two theoretical properties for the Nitsche-based method (5): consistency and well-posedness. These properties, together with optimal *a priori* error estimates in $H^1(\Omega)$-norm, are proven in [16].

Like Nitsche's method for second order elliptic problems with Dirichlet boundary conditions or domain decomposition [5], our Nitsche-based formulation (5) for unilateral contact is consistent:

Lemma 2.4. *The Nitsche-based method for contact is consistent: suppose that the solution* $\mathbf{u}$ *of (1)–(2) lies in* $(H^{\frac{3}{2}+\nu}(\Omega))^d$ *with* $\nu > 0$ *and* $d = 2, 3$. *Then* $\mathbf{u}$ *is also solution of*

$$A_{\theta\gamma}(\mathbf{u}, \mathbf{v}^h) + \int_{\Gamma_C} \frac{1}{\gamma} \left[P_\gamma(\mathbf{u})\right]_+ P_{\theta\gamma}(\mathbf{v}^h) \, d\Gamma = L(\mathbf{v}^h), \quad \forall \mathbf{v}^h \in \mathbf{V}^h.$$

Problem (5) is well-posed in the following sense and under the assumptions below:

Theorem 2.5. *Suppose that either* $\theta \neq -1$ *and* $\gamma_0 > 0$ *is sufficiently small, or* $\theta = -1$ *and* $\gamma_0 > 0$. *Then Problem* (5) *admits one unique solution* $\mathbf{u}^h$ *in* $\mathbf{V}^h$.

Remark 2.6. *When* γ_0 *is large and* $\theta \neq -1$ *we can neither conclude to uniqueness, nor to existence of a solution. In reference [16] there are some simple explicit examples of nonexistence and nonuniqueness of solutions.*

3 *A posteriori* error analysis

3.1 Definition of the residual error estimator

The element residual of the equilibrium equation in (1) is defined by

$$\mathbf{div}\,\boldsymbol{\sigma}(\mathbf{u}^h) + \mathbf{f} \text{ in } K.$$

Remark 3.1. *For linear elements* $(k = 1)$, *the term* $\mathbf{div}\,\boldsymbol{\sigma}(\mathbf{u}^h)$ *vanishes.*

As usual this element residual can be replaced by some finite dimensional approximation, called approximate element residual (see, e.g., [2])

$$\mathbf{div}\,\boldsymbol{\sigma}(\mathbf{u}^h) + \mathbf{f}_K, \quad \mathbf{f}_K \in (P_l(K))^d, \quad l \geq 0.$$

A current choice is to take $\mathbf{f}_K = \displaystyle\int_K \mathbf{f}(\boldsymbol{x})\,/|K|\,d\boldsymbol{x}$ since for $\mathbf{f} \in (H^1(\Omega))^d$, scaling arguments yield $\|\mathbf{f} - \mathbf{f}_K\|_{0,K} \lesssim h_K \|\mathbf{f}\|_{1,K}$ and it is then negligible with respect to the estimator η defined hereafter. In the same way $\mathbf{g}$ is approximated by a computable quantity denoted $\mathbf{g}_E$ on any $E \in E_h^N$.

Definition 3.2. *The local error estimators η_K and the the global estimator η are defined by*

$$\eta_K = \left(\sum_{i=1}^{4} \eta_{iK}^2 \right)^{1/2},$$

$$\eta_{1K} = h_K \|\mathbf{div}\,\boldsymbol{\sigma}(\mathbf{u}^h) + \mathbf{f}_K\|_{0,K},$$

$$\eta_{2K} = h_K^{1/2} \left(\sum_{E \in E_K^{int} \cup E_K^N} \|J_{E,n}(\mathbf{u}^h)\|_{0,E}^2 \right)^{1/2},$$

$$\eta_{3K} = h_K^{1/2} \left(\sum_{E \in E_K^C} \|\boldsymbol{\sigma_t}(\mathbf{u}^h)\|_{0,E}^2 \right)^{1/2},$$

$$\eta_{4K} = h_K^{1/2} \left(\sum_{E \in E_K^C} \left\| \frac{1}{\gamma}[P_\gamma(\mathbf{u}^h)]_+ + \sigma_n(\mathbf{u}^h) \right\|_{0,E}^2 \right)^{1/2},$$

$$\eta = \left(\sum_{K \in T_h} \eta_K^2 \right)^{1/2},$$

where $J_{E,n}(\mathbf{u}^h)$ means the constraint jump of $\mathbf{u}^h$ in the normal direction, i.e.,

$$J_{E,n}(\mathbf{u}^h) = \begin{cases} [\![\boldsymbol{\sigma}(\mathbf{u}^h)\boldsymbol{\nu}_E]\!]_E, & \forall E \in E_h^{int}, \\ \boldsymbol{\sigma}(\mathbf{u}^h)\boldsymbol{\nu}_E - \mathbf{g}_E, & \forall E \in E_h^N. \end{cases} \tag{10}$$

The local and global approximation terms are given by

$$\zeta_K = \left(h_K^2 \sum_{K' \subset \omega_K} \|\mathbf{f} - \mathbf{f}_{K'}\|_{0,K'}^2 + h_E \sum_{E \subset E_K^N} \|\mathbf{g} - \mathbf{g}_E\|_{0,E}^2 \right)^{1/2},$$

$$\zeta = \left(\sum_{K \in T_h} \zeta_K^2 \right)^{1/2}.$$

3.2   Upper error bound

First we state a "saturation" assumption that we need in order to prove the estimate (see also [5] in the case of Nitsche for domain decomposition, and [49] for mortar methods).

Assumption 3.3. *The solution $\mathbf{u}$ of (3) and the discrete solution $\mathbf{u}^h$ of (5) are such that:*

$$\left\| \sigma_n(\mathbf{u} - \mathbf{u}^h) \right\|_{-1/2,h,\Gamma_C} \lesssim \|\mathbf{u} - \mathbf{u}^h\|_{1,\Omega}. \tag{11}$$

Remark 3.4. *Note that for a Nitsche's treatment of (linear) interface conditions, an upper bound for a residual-based estimator has been derived without such an assumption in [27]. Similarly for some classes of mixed non-conforming finite element approximations, an assumption such as 3.3 has revealed to be superfluous, see, e.g., references [12, 36]. However for the method (5) the derivation of an upper bound without such kind of saturation assumption remains an open issue.*

The following statement guarantees the reliability of the *a posteriori* error estimator given in Definition 3.2:

Theorem 3.5. *Let* $\mathbf{u}$ *be the solution to the variational inequality (3), with* $\mathbf{u} \in (H^{\frac{3}{2}+\nu}(\Omega))^d$ *($\nu > 0$ and $d = 2,3$), and let* $\mathbf{u}^h$ *be the solution to the corresponding discrete problem (5). Assume that, for $\theta \neq -1$, γ_0 is sufficiently small, and otherwise that $\gamma_0 > 0$ for $\theta = -1$. Assume that the saturation assumption (11) holds as well. Then we have*

$$\|\mathbf{u} - \mathbf{u}^h\|_{1,\Omega} + \left\| \sigma_n(\mathbf{u}) + \frac{1}{\gamma}[P_\gamma(\mathbf{u}^h)]_+ \right\|_{-1/2,h,\Gamma_C} + \|\sigma_n(\mathbf{u}) - \sigma_n(\mathbf{u}^h)\|_{-1/2,h,\Gamma_C} \lesssim (1 + \gamma_0)\eta + \zeta.$$

Proof: Let $\mathbf{v}^h \in \mathbf{V}^h$. To lighten the notation, we denote $\mathbf{e} := \mathbf{u} - \mathbf{u}^h$. We first use the **V**-ellipticity of $a(\cdot, \cdot)$, together with the Green formula, equations (1) and (5) to obtain:

$$\begin{aligned}
\alpha \|\mathbf{e}\|^2_{1,\Omega} &\leq a(\mathbf{u} - \mathbf{u}^h, \mathbf{u} - \mathbf{u}^h) \\
&= a(\mathbf{u}, \mathbf{u} - \mathbf{u}^h) - a(\mathbf{u}^h, \mathbf{u} - \mathbf{v}^h) - a(\mathbf{u}^h, \mathbf{v}^h - \mathbf{u}^h) \\
&= L(\mathbf{u} - \mathbf{u}^h) + \int_{\Gamma_C} \sigma_n(\mathbf{u})(u_n - u_n^h) \, d\Gamma - a(\mathbf{u}^h, \mathbf{u} - \mathbf{v}^h) \\
&\quad - L(\mathbf{v}^h - \mathbf{u}^h) + \int_{\Gamma_C} \frac{1}{\gamma}[P_\gamma(\mathbf{u}^h)]_+ P_{\theta\gamma}(\mathbf{v}^h - \mathbf{u}^h) \, d\Gamma - \theta \int_{\Gamma_C} \gamma \, \sigma_n(\mathbf{u}^h)\sigma_n(\mathbf{v}^h - \mathbf{u}^h) \, d\Gamma \\
&= \mathcal{T}_1 + \mathcal{T}_2 \tag{12}
\end{aligned}$$

where α is the **V**$-$ellipticity constant of $a(\cdot, \cdot)$ and

$$\mathcal{T}_1 := L(\mathbf{u} - \mathbf{v}^h) - a(\mathbf{u}^h, \mathbf{u} - \mathbf{v}^h) + \int_{\Gamma_C} \frac{1}{\gamma}[P_\gamma(\mathbf{u}^h)]_+(v_n^h - u_n) \, d\Gamma$$

$$\begin{aligned}
\mathcal{T}_2 &:= \int_{\Gamma_C} \sigma_n(\mathbf{u})(u_n - u_n^h) \, d\Gamma + \int_{\Gamma_C} \frac{1}{\gamma}[P_\gamma(\mathbf{u}^h)]_+ P_{\theta\gamma}(\mathbf{u} - \mathbf{u}^h) \, d\Gamma \\
&\quad - \theta \int_{\Gamma_C} \frac{1}{\gamma}[P_\gamma(\mathbf{u}^h)]_+ \gamma \sigma_n(\mathbf{v}^h - \mathbf{u}) \, d\Gamma - \theta \int_{\Gamma_C} \gamma \, \sigma_n(\mathbf{u}^h)\sigma_n(\mathbf{v}^h - \mathbf{u}^h) \, d\Gamma.
\end{aligned}$$

The quantity $\mathcal{T}_1$ is an expression which is handled hereafter in a classical way. Namely, by integrating by parts on each triangle K, using the definition of $J_{E,n}(\mathbf{u}^h)$ in (10) and splitting up the integrals on Γ_C into normal and tangential components we get:

$$\begin{aligned}
\mathcal{T}_1 &= \sum_{K \in T_h} \int_K (\mathbf{div}\, \boldsymbol{\sigma}(\mathbf{u}^h) + \mathbf{f}) \cdot (\mathbf{u} - \mathbf{v}^h) \, d\Gamma \\
&\quad + \sum_{E \in E_h^C} \int_E \left(\frac{1}{\gamma}[P_\gamma(\mathbf{u}^h)]_+ + \sigma_n(\mathbf{u}^h) \right)(v_n^h - u_n) \, d\Gamma \\
&\quad + \sum_{E \in E_h^C} \int_E \boldsymbol{\sigma_t}(\mathbf{u}^h) \cdot (\mathbf{v_t}^h - \mathbf{u_t}) \, d\Gamma - \sum_{E \in E_h^{int} \cup E_h^N} \int_E J_{E,n}(\mathbf{u}^h) \cdot (\mathbf{u} - \mathbf{v}^h) \, d\Gamma \\
&\quad + \sum_{E \in E_h^N} \int_E (\mathbf{g} - \mathbf{g}_E) \cdot (\mathbf{u} - \mathbf{v}^h) \, d\Gamma. \tag{13}
\end{aligned}$$

We now need to estimate each term of this right-hand side. For that purpose, we take

$$\mathbf{v}^h = \mathbf{u}^h + R^h(\mathbf{u} - \mathbf{u}^h), \tag{14}$$

8

where R^h is the quasi-interpolation operator defined in Section 2.2.

We start with the integral term on elements K. Cauchy-Schwarz's inequality implies

$$\sum_{K \in T_h} \int_K (\mathbf{div}\, \boldsymbol{\sigma}(\mathbf{u}^h) \,+\, \mathbf{f}) \cdot (\mathbf{u} - \mathbf{v}^h) \, d\Gamma \leq \sum_{K \in T^h} \|\mathbf{div}\, \boldsymbol{\sigma}(\mathbf{u}^h) \,+\, \mathbf{f}\|_{0,K} \|\mathbf{u} - \mathbf{v}^h\|_{0,K},$$

and it suffices to estimate $\|\mathbf{u} - \mathbf{v}^h\|_{0,K}$ for any triangle K. From the definition of $\mathbf{v}^h$ and (6) we get:

$$\|\mathbf{u} - \mathbf{v}^h\|_{0,K} = \|\mathbf{e} - R^h \mathbf{e}\|_{0,K} \lesssim h_K \|\mathbf{e}\|_{1,\omega_K}.$$

As a consequence

$$\left| \int_\Omega (\mathbf{div}\, \boldsymbol{\sigma}(\mathbf{u}^h) \,+\, \mathbf{f}) \cdot (\mathbf{u} - \mathbf{v}^h) \, d\Gamma \right| \lesssim (\eta + \zeta) \|\mathbf{e}\|_{1,\Omega}.$$

We now consider the interior and Neumann boundary terms in (13). As we previously noticed, the application of Cauchy-Schwarz's inequality leads to

$$\left| \sum_{E \in E_h^{int} \cup E_h^N} \int_E J_{E,n}(\mathbf{u}^h) \cdot (\mathbf{u} - \mathbf{v}^h) \, d\Gamma \right| \leq \sum_{E \in E_h^{int} \cup E_h^N} \|J_{E,n}(\mathbf{u}^h)\|_{0,E} \|\mathbf{u} - \mathbf{v}^h\|_{0,E}.$$

Therefore using expression (14) and estimate (7), we obtain

$$\|\mathbf{u} - \mathbf{v}^h\|_{0,E} = \|\mathbf{e} - R^h \mathbf{e}\|_{0,E} \lesssim h_E^{1/2} \|\mathbf{e}\|_{1,\omega_E}.$$

Inserting this estimate in the previous one we deduce that

$$\left| \sum_{E \in E_h^{int} \cup E_h^N} \int_E J_{E,n}(\mathbf{u}^h) \cdot (\mathbf{u} - \mathbf{v}^h) \, d\Gamma \right| \lesssim \eta \|\mathbf{e}\|_{1,\Omega}.$$

Moreover,

$$\left| \sum_{E \in E_h^N} \int_E (\mathbf{g} - \mathbf{g}_E) \cdot (\mathbf{u} - \mathbf{v}^h) \, d\Gamma \right| \lesssim \zeta \|\mathbf{e}\|_{1,\Omega}.$$

The two following terms are handled in a similar way as the previous ones so that

$$\left| \sum_{E \in E_h^C} \int_E \left(\frac{1}{\gamma} [P_\gamma(\mathbf{u}^h)]_+ + \sigma_n(\mathbf{u}^h) \right) (v_n^h - u_n) \, d\Gamma \right| \lesssim \eta \|\mathbf{e}\|_{1,\Omega},$$

and

$$\left| \sum_{E \in E_h^C} \int_E \boldsymbol{\sigma}_\mathbf{t}(\mathbf{u}^h) \cdot (\mathbf{v}_\mathbf{t}^h - \mathbf{u}_\mathbf{t}) \, d\Gamma \right| \lesssim \eta \|\mathbf{e}\|_{1,\Omega}.$$

Collecting the previous results, we deduce:

$$\mathcal{T}_1 \lesssim (\eta + \zeta) \|\mathbf{e}\|_{1,\Omega}. \tag{15}$$

The first two terms in $\mathcal{T}_2$ are split using the definition of $P_\gamma(\cdot)$ and $P_{\theta\gamma}(\cdot)$, and the last one is split using relationship $\sigma_n(\mathbf{v}^h - \mathbf{u}^h) = \sigma_n((\mathbf{v}^h - \mathbf{u}) + (\mathbf{u} - \mathbf{u}^h))$. This leads to:

$$\mathcal{T}_2 = \int_{\Gamma_C} \sigma_n(\mathbf{u}) P_\gamma(\mathbf{u} - \mathbf{u}^h)\, d\Gamma + \int_{\Gamma_C} \sigma_n(\mathbf{u})\gamma\sigma_n(\mathbf{u} - \mathbf{u}^h)\, d\Gamma$$
$$+ \int_{\Gamma_C} \frac{1}{\gamma}[P_\gamma(\mathbf{u}^h)]_+ P_\gamma(\mathbf{u} - \mathbf{u}^h)\, d\Gamma + (1-\theta)\int_{\Gamma_C} \frac{1}{\gamma}[P_\gamma(\mathbf{u}^h)]_+ \gamma\sigma_n(\mathbf{u} - \mathbf{u}^h)\, d\Gamma$$
$$- \theta\int_{\Gamma_C} \frac{1}{\gamma}\left([P_\gamma(\mathbf{u}^h)]_+ + \sigma_n(\mathbf{u}^h)\right)\gamma\sigma_n(\mathbf{v}^h - \mathbf{u})\, d\Gamma - \theta\int_{\Gamma_C} \gamma\,\sigma_n(\mathbf{u}^h)\sigma_n(\mathbf{u} - \mathbf{u}^h)\, d\Gamma.$$

Then we split the second term in the above expression using $1 = \theta + (1-\theta)$ and we gather the resulting terms:

$$\mathcal{T}_2 = \int_{\Gamma_C}\left(\frac{1}{\gamma}[P_\gamma(\mathbf{u}^h)]_+ + \sigma_n(\mathbf{u})\right)P_\gamma(\mathbf{u} - \mathbf{u}^h)\, d\Gamma + (1-\theta)\int_{\Gamma_C}\frac{1}{\gamma}\left(\sigma_n(\mathbf{u}) + [P_\gamma(\mathbf{u}^h)]_+\right)\gamma\sigma_n(\mathbf{u} - \mathbf{u}^h)\, d\Gamma$$
$$- \theta\int_{\Gamma_C}\left(\frac{1}{\gamma}[P_\gamma(\mathbf{u}^h)]_+ + \sigma_n(\mathbf{u}^h)\right)\gamma\sigma_n(\mathbf{v}^h - \mathbf{u})\, d\Gamma + \theta\|\gamma^{1/2}\sigma_n(\mathbf{u} - \mathbf{u}^h)\|_{0,\Gamma_C}^2.$$

Now we substitute $\sigma_n(\mathbf{u})$ using the reformulation of contact conditions (2) (i)-(iii) as $\sigma_n(\mathbf{u}) = -\frac{1}{\gamma}[P_\gamma(\mathbf{u})]_+$ (see for instance [3, 15]). This reformulation makes sense in $L^2(\Gamma_C)$ due to the regularity assumption $\mathbf{u} \in (H^{\frac{3}{2}+\nu}(\Omega))^d$. Afterwards we apply the bound (4) in the first term as well as Cauchy-Schwarz inequality in the second one:

$$\mathcal{T}_2 \leq -\|\gamma^{\frac{1}{2}}(\sigma_n(\mathbf{u}) + \frac{1}{\gamma}[P_\gamma(\mathbf{u}^h)]_+)\|_{0,\Gamma_C}^2 + |\theta - 1|\|\gamma^{\frac{1}{2}}(\sigma_n(\mathbf{u}) + \frac{1}{\gamma}[P_\gamma(\mathbf{u}^h)]_+)\|_{0,\Gamma_C}\|\gamma^{1/2}\sigma_n(\mathbf{u} - \mathbf{u}^h)\|_{0,\Gamma_C}$$
$$- \theta\int_{\Gamma_C}\left(\frac{1}{\gamma}[P_\gamma(\mathbf{u}^h)]_+ + \sigma_n(\mathbf{u}^h)\right)\gamma\sigma_n(\mathbf{v}^h - \mathbf{u})\, d\Gamma + \theta\|\gamma^{1/2}\sigma_n(\mathbf{u} - \mathbf{u}^h)\|_{0,\Gamma_C}^2.$$

The expression $ab \leq a^2 + b^2/4$ yields, for any $\beta > 0$:

$$\mathcal{T}_2 \leq \frac{|\theta-1|^2}{4}\|\gamma^{1/2}\sigma_n(\mathbf{u} - \mathbf{u}^h)\|_{0,\Gamma_C}^2$$
$$- \theta\int_{\Gamma_C}\left(\frac{1}{\gamma}[P_\gamma(\mathbf{u}^h)]_+ + \sigma_n(\mathbf{u}^h)\right)\gamma\sigma_n(\mathbf{v}^h - \mathbf{u})\, d\Gamma + \theta\|\gamma^{1/2}\sigma_n(\mathbf{u} - \mathbf{u}^h)\|_{0,\Gamma_C}^2$$
$$= \frac{(\theta+1)^2}{4}\|\gamma^{1/2}\sigma_n(\mathbf{u} - \mathbf{u}^h)\|_{0,\Gamma_C}^2 - \theta\int_{\Gamma_C}\left(\frac{1}{\gamma}[P_\gamma(\mathbf{u}^h)]_+ + \sigma_n(\mathbf{u}^h)\right)\gamma\sigma_n(\mathbf{v}^h - \mathbf{u})\, d\Gamma$$
$$\leq \frac{(\theta+1)^2}{4}\|\gamma^{1/2}\sigma_n(\mathbf{u} - \mathbf{u}^h)\|_{0,\Gamma_C}^2 + |\theta|\gamma_0^{1/2}\eta\|\gamma^{1/2}\sigma_n(\mathbf{v}^h - \mathbf{u})\|_{0,\Gamma_C}$$
$$\leq \frac{(\theta+1)^2}{4}\|\gamma^{1/2}\sigma_n(\mathbf{u} - \mathbf{u}^h)\|_{0,\Gamma_C}^2 + \beta\theta^2\gamma_0\eta^2 + \frac{1}{2\beta}\|\gamma^{1/2}\sigma_n(\mathbf{v}^h - \mathbf{u}^h)\|_{0,\Gamma_C}^2 + \frac{1}{2\beta}\|\gamma^{1/2}\sigma_n(\mathbf{u}^h - \mathbf{u})\|_{0,\Gamma_C}^2$$
$$= \left(\frac{1}{2\beta} + \frac{(\theta+1)^2}{4}\right)\gamma_0\|\sigma_n(\mathbf{u} - \mathbf{u}^h)\|_{-1/2,h,\Gamma_C}^2 + \beta\theta^2\gamma_0\eta^2 + \frac{\gamma_0}{2\beta}\|\sigma_n(\mathbf{v}^h - \mathbf{u}^h)\|_{-1/2,h,\Gamma_C}^2.$$

Using (9) and the H^1-stability of R^h (see (8) in Lemma 2.1) we bound:

$$\|\sigma_n(\mathbf{v}^h - \mathbf{u}^h)\|_{-1/2,h,\Gamma_C} \leq C\|\mathbf{v}^h - \mathbf{u}^h\|_{1,\Omega} = C\|R^h(\mathbf{u} - \mathbf{u}^h)\|_{1,\Omega} \leq C\|\mathbf{u} - \mathbf{u}^h\|_{1,\Omega}.$$

We combine this last bound with the saturation assumption (11) and get

$$\mathcal{T}_2 \leq C\gamma_0 \left(\frac{(\theta+1)^2}{4} + \frac{1}{\beta} \right) \|\mathbf{u} - \mathbf{u}^h\|_{1,\Omega}^2 + \beta\theta^2\gamma_0\eta^2. \tag{16}$$

Now we combine estimates (12), (15) and (16):

$$\alpha\|\mathbf{e}\|_{1,\Omega}^2 \leq C(\eta+\zeta)\|\mathbf{e}\|_{1,\Omega} + C\gamma_0 \left(\frac{(\theta+1)^2}{4} + \frac{1}{\beta} \right) \|\mathbf{e}\|_{1,\Omega}^2 + \beta\theta^2\gamma_0\eta^2.$$

We treat the first term on the right-hand side with Young's inequality and obtain:

$$\left(\frac{\alpha}{2} - C\gamma_0 \left(\frac{(\theta+1)^2}{4} + \frac{1}{\beta} \right) \right) \|\mathbf{e}\|_{1,\Omega}^2 \leq \frac{C}{\alpha}(\eta^2 + \zeta^2) + \beta\theta^2\gamma_0\eta^2.$$

When $\theta \neq -1$, we choose γ_0 sufficiently small, and for $\theta = -1$, we can choose for instance $\beta = \frac{4C\gamma_0}{\alpha}$ (for a fixed value of $\gamma_0 > 0$, that does not need to be small in this case). We obtain the upper bound on the error in natural norm:

$$\|\mathbf{e}\|_{1,\Omega} \lesssim (1 + \gamma_0)\eta + \zeta.$$

The saturation assumption (11) provides directly a bound on the contact stress error:

$$\|\sigma_n(\mathbf{u} - \mathbf{u}^h)\|_{-1/2,h,\Gamma_C} \lesssim \|\mathbf{e}\|_{1,\Omega}.$$

For the contact error we make use of the triangle inequality, and of the above inequality:

$$\left\| \sigma_n(\mathbf{u}) + \frac{1}{\gamma}[P_\gamma(\mathbf{u}^h)]_+ \right\|_{-1/2,h,\Gamma_C} \leq \|\sigma_n(\mathbf{u} - \mathbf{u}^h)\|_{-1/2,h,\Gamma_C} + \left\| \sigma_n(\mathbf{u}^h) + \frac{1}{\gamma}[P_\gamma(\mathbf{u}^h)]_+ \right\|_{-1/2,h,\Gamma_C}$$
$$\lesssim \|\mathbf{e}\|_{1,\Omega} + \eta.$$

Collecting the three previous results allows to prove the theorem. $\qquad\square$

3.3 Lower error bound

We now consider the local lower error bounds of the discretization error terms.

Theorem 3.6. *For all elements $K \in T_h$, the following local lower error bounds hold:*

$$\eta_{1K} \lesssim \|\mathbf{u} - \mathbf{u}^h\|_{1,K} + \zeta_K, \tag{17}$$
$$\eta_{2K} \lesssim \|\mathbf{u} - \mathbf{u}^h\|_{1,\omega_K} + \zeta_K. \tag{18}$$

For all elements K such that $K \cap E_h^C \neq \emptyset$, the following local lower error bounds hold:

$$\eta_{3K} \lesssim \|\mathbf{u} - \mathbf{u}^h\|_{1,K} + \zeta_K, \tag{19}$$

$$\eta_{4K} \lesssim \sum_{E \in E_K^C} h_K^{1/2} \left(\left\| \sigma_n(\mathbf{u}) + \frac{1}{\gamma}[P_\gamma(\mathbf{u}^h)]_+ \right\|_{0,E} + \left\| \sigma_n(\mathbf{u} - \mathbf{u}^h) \right\|_{0,E} \right). \tag{20}$$

Proof: The estimates of η_{1K}, η_{2K} in (17)–(18) are standard (see, e.g., [47]). The estimate η_{3K} in (19) is handled in a standard way as in [31].

The estimate of η_{4K} in (20) is obtained from the Definition 3.2 and triangular inequality. $\quad\square$

Remark 3.7. *Remark that, from Theorem 3.6, optimal convergence rates of order $O(h^{\min(k,\frac{1}{2}+\nu)})$ are expected for the estimator of Definition 3.2.*

Remark 3.8. *An extension of the above analysis for the Tresca friction case is sketched in Appendix 1.*

4 Numerical experiments

We illustrate numerically the theoretical properties of the error estimator η given in Definition 3.2 and compute its convergence order when h vanishes. To study separately global contributions of each component of η we introduce the notation

$$\eta_i = \left(\sum_{K \in T_h} \eta_{iK}^2 \right)^{1/2} \qquad 1 \leq i \leq 4,$$

where the expressions of η_{iK} are provided in Definition 3.2. In all examples below Hooke's law is considered: E and ν_P will denote respectively Young's modulus and Poisson's ratio. Moreover a dimensional analysis allows to deduce that γ_0 is the inverse of a stiffness parameter. Consequently we choose in our discussion $\gamma_0 = C/E$ where C is a constant which does not depend on E. The finite element method (5) as well as the residual estimator η are implemented under the open source finite element library GetFEM++[1]. For details on numerical solving we refer to [16, 44].

To measure the quality of the estimator η we introduce the effectivity index:

$$eff_E = \frac{\eta}{E \left\| \mathbf{u} - \mathbf{u}^h \right\|_{1,\Omega}}.$$

As in [31] this index has been normalized with respect to Young's modulus E. Indeed, we remark that if $\mathbf{u}(E)$ denotes the solution of a (linear) Lamé system with a Young modulus E then $\mathbf{u}(mE) = \mathbf{u}(E)/m$ whereas $\sigma(\mathbf{u}(mE)) = \sigma(\mathbf{u}(E))$. Thus the error estimator η is independent of E (for η_4 this property comes from the scaling $\gamma_0 = C/E$). In contrast there holds $\left\| \mathbf{u}(mE) - \mathbf{u}^h(mE) \right\|_{1,\Omega} = \left\| \mathbf{u}(E) - \mathbf{u}^h(E) \right\|_{1,\Omega}/m$ that becomes independent of E for the choice $m = 1/E$.

4.1 First example: a square with slip and separation

4.1.1 Description

We first consider a test case taken from [31] (see also [29, 41] in the frictional case). We consider the domain $\Omega = (0,1) \times (0,1)$ with material characteristics $E = 10^6$ and $\nu_P = 0.3$. A homogeneous Dirichlet condition on $\Gamma_D = \{0\} \times (0,1)$ is prescribed to clamp the body. The body is potentially in contact on $\Gamma_C = \{1\} \times (0,1)$ with a rigid obstacle and $\Gamma_N = (0,1) \times (\{0\} \cup \{1\})$ is the location of a homogeneous Neumann condition. The body Ω is acted on by a vertical volume density of force $\mathbf{f} = (0, f_2)$ with $f_2 = -76518$ such that there is coexistence of a slip zone and a separation zone with a transition point between both zones. For error computations, since we do not have a closed-form solution, a reference solution is computed with Lagrange P_2 elements, $h = 1/160$, $\gamma_0 = 1/E$ and $\theta = -1$.

First of all we illustrate in Figure 1 the difference between uniform and adaptive refinement. For the latter we refine only the mesh elements K in which the local estimator η_K is below a given threshold $s = 2.5 \times 10^{-3}$. The minimal (respectively maximal) size of the adaptive mesh is equal to $1/160$ (respectively $h = 1/40$). As expected the rate of convergence with respect to the number of degrees of freedom is far better in the case of adaptive refinement than with uniform refinement.

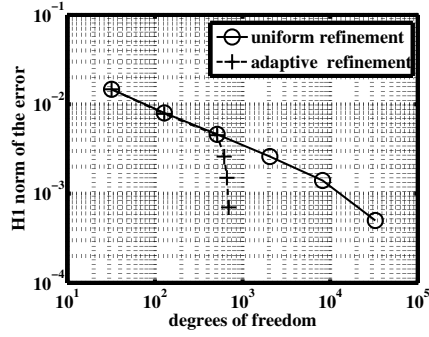
[1]see http://download.gna.org/getfem/html/homepage/

Figure 1: Rate of convergence for uniform and adaptive refinement methods. Parameters $\gamma_0 = 1/E$, $\theta = -1$ and Lagrange P_2 elements.

Figure 2: Left panel: mesh with adaptive refinement and contact boundary on the right. Right panel: plot of Von Mises stress. Parameters $\gamma_0 = 1/E$, $\theta = -1$ and Lagrange P_2 elements.
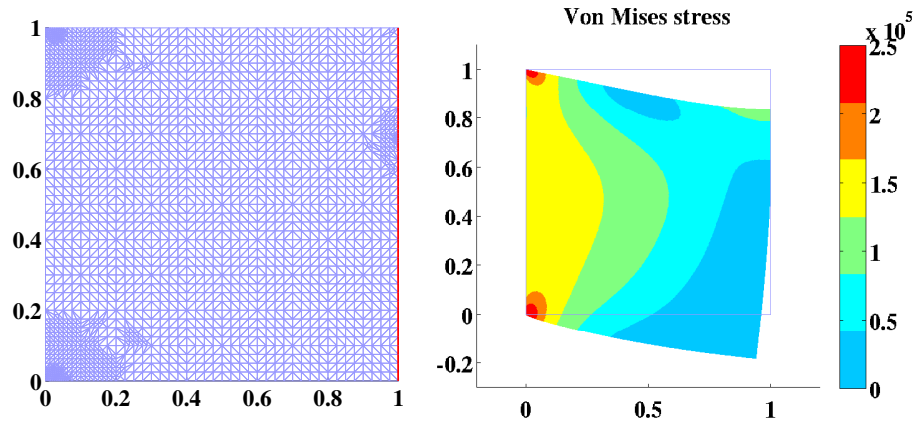

Figure 3: Left panel: mesh with adaptive refinement and contact boundary on the right. Right panel: plot of Von Mises stress. Parameters $\gamma_0 = 1/E$, $\theta = 1$ and Lagrange P_2 elements.

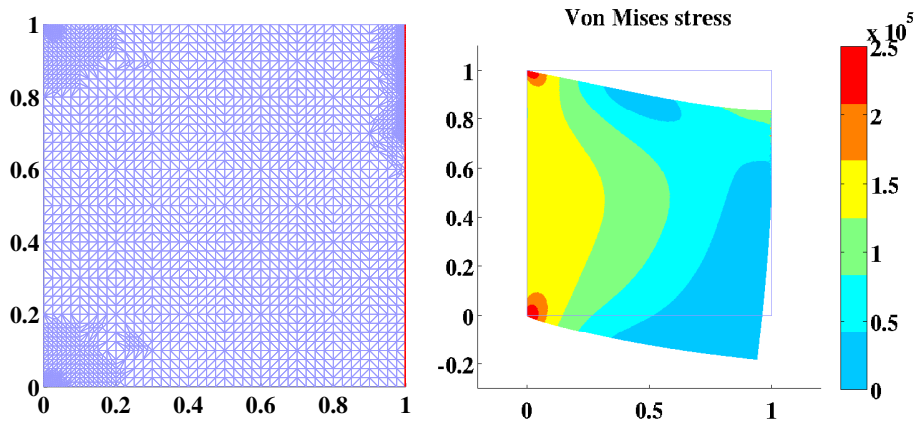The solution obtained with adaptive refinement and $\theta = -1$ is depicted in Figure 2. We observe that the error is concentrated at both left corners (transition between Dirichlet and Neumann conditions) and near the transition point between contact and separation. As expected

13

we observe that all the nodes on Γ_C have a negative tangential displacement and that Γ_C is divided into two parts: the upper part where the body remains in contact (slipping nodes) and the lower part where it is separated, with a transition point near $(1, 0.685)$. The value is close to the transition point $(1, 0.69 \pm 0.01)$ found in [31] and $(1, 0.65)$ found in [41]. The slight difference with [41] should be due to Coulomb friction.

Remark 4.1. *Note that the solution in the case $\theta = 1$ (see Figure 3) has an error estimator on the contact zone which is larger than in the case $\theta = -1$. In the case $\theta = -1$, the discrete solution is less dependent on the parameter γ_0 than for the other methods (see [16]) and we obtain a better approximation of the problem on the contact boundary Γ_C.*

4.1.2   Numerical convergence

We perform a numerical convergence study for three variants of method (5) corresponding to $\theta = 1$, $\theta = 0$ and $\theta = -1$. The Nitsche parameter γ_0 is fixed to $1/E$, which should ensure well-posedness and optimal convergence in each case. Lagrange P_1 finite elements are chosen. The reference solution for error computations corresponds to the one described in Section 4.1.1 and depicted in Figure 2 (P_2 finite elements, $\theta = -1$ and adaptive finest mesh). No mesh adaptation is carried out anymore and only uniform refinement is imposed, with a sequence of decreasing mesh sizes h.

First the estimator η, the L^2 and the H^1-norms of the error $\mathbf{u} - \mathbf{u}^h$ are depicted in Figure 4. One can note a sub-optimality of the convergence rate in L^2 and H^1-norms of the error. They are caused by the Neumann-Dirichlet transition on the left corners of Ω (the same observation has been reported in [23]).
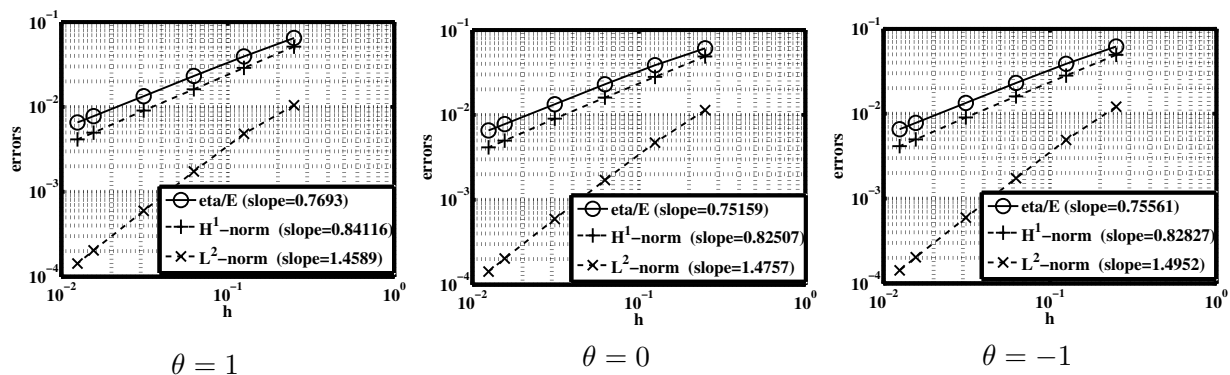

$\theta = 1 \qquad\qquad\qquad \theta = 0 \qquad\qquad\qquad \theta = -1$

Figure 4: First example. Convergence curves of the error estimator η, the L^2 and H^1-norms of the error $\mathbf{u} - \mathbf{u}^h$, for $\gamma_0 = 1/E$.

Then the different contributions of η are reported on Tables 1, 2 and 3. The convergence rate of η_1 is strictly equal to 1 since, for piecewise linear finite elements, the expression of this estimator reduces to $\eta_{1K} = h_K \|\mathbf{f}_K\|_{0,K}$. More generally, all the estimators η_i converge towards zero as h vanishes, and they behave identically whatever the value of θ is (this is due to the low value of γ_0). Moreover, the convergence rate of η_2 is slightly less than the one of the H^1-norm of the error whereas the convergence rates of η_3 and η_4 are far greater, and higher than 1 (we do not have a clear interpretation of this). In all cases, we obtain an effectivity index between 1.2 and 1.6 (the average is close to 1.45 and the standard deviation is close to 0.12). These overall results are quite similar to those presented in [31, 41].

Table 1: First example, $\theta = 1$ and $\gamma_0 = 1/E$.

Mesh size h	1/4	1/8	1/16	1/32	1/64	1/80	slope
Degrees of freedom	32	128	512	2048	8192	12800	
$\|\mathbf{u} - \mathbf{u}^h\|_{0,\Omega}$ ($\times 10^{-4}$)	104.7551	48.2436	17.3689	5.9666	2.0366	1.4262	1.4589
$\|\mathbf{u} - \mathbf{u}^h\|_{1,\Omega}$ ($\times 10^{-3}$)	51.3896	28.8563	16.1335	9.0627	4.9777	4.1489	0.8412
η_1	16719.8	8359.9	4179.95	2089.97	1044.99	835.99	1.0000
η_2	60779.5	38076.7	22698	13222.3	7724.01	6507.89	0.7522
η_3	7626.32	3209.18	1207.19	427.694	157.242	118.467	1.4107
η_4	13501	4604.89	1395.58	370.912	100.73	77.2	1.7646
η	64916.4	39385.6	23153.3	13398.4	7796.61	6562.89	0.7779
Effectivity index Eff_E	1.2632	1.3649	1.4351	1.4784	1.5661	1.5816	

Table 2: First example, $\theta = 0$ and $\gamma_0 = 1/E$.

Mesh size h	1/4	1/8	1/16	1/32	1/64	1/80	slope
Degrees of freedom	32	128	512	2048	8192	12800	
$\|\mathbf{u} - \mathbf{u}^h\|_{0,\Omega}$ ($\times 10^{-4}$)	113.6807	47.1350	17.0780	5.9262	2.0312	1.4229	1.4757
$\|\mathbf{u} - \mathbf{u}^h\|_{1,\Omega}$ ($\times 10^{-3}$)	48.8181	28.0213	15.9877	9.0359	4.9716	4.1459	0.8251
η_1	16719.8	8359.9	4179.95	2089.97	1044.99	835.99	1.0000
η_2	57305.3	37374.7	22547.2	13200.7	7720.86	6505.24	0.7356
η_3	3938.22	1852.35	720.951	256.135	95.0474	71.047	1.3686
η_4	11946.5	4002.56	1154.11	324.915	89.6552	61.026	1.7809
η	61005.6	38551.4	22971.7	13371.5	7792.35	6559.4	0.7779
Effectivity index Eff_E	1.2496	1.3758	1.4368	1.4798	1.5672	1.5819	

Table 3: First example, $\theta = -1$ and $\gamma_0 = 1/E$.

Mesh size h	1/4	1/8	1/16	1/32	1/64	1/80	slope
Degrees of freedom	32	128	512	2048	8192	12800	
$\|\mathbf{u} - \mathbf{u}^h\|_{0,\Omega}$ ($\times 10^{-4}$)	120.9371	48.9718	17.3613	5.9619	2.0360	1.4255	1.4952
$\|\mathbf{u} - \mathbf{u}^h\|_{1,\Omega}$ ($\times 10^{-3}$)	49.3705	28.1269	16.0087	9.0385	4.9714	4.1467	0.8283
η_1	16719.8	8359.9	4179.95	2089.97	1044.99	835.99	1.0000
η_2	58846.3	37649.9	22607.7	13213.2	7723.58	6506.99	0.7428
η_3	2690.5	1464.81	558.637	192.194	70.7559	53.7733	1.3544
η_4	9202.06	2854.93	832.228	229.683	62.842	44.0949	1.8004
η	61922.2	38700.1	23012.7	13380.8	7794.52	6560.84	0.7779
Effectivity index Eff_E	1.2542	1.3759	1.4375	1.4804	1.5677	1.5820	

On Figure 5 the numerical experiment is performed for a larger parameter $\gamma_0 = 1000/E$. In the case $\theta = 1$ and in the case $\theta = 0$ the convergence rate is degraded compared to the case $\gamma_0 = 1/E$. Conversely, in the case $\theta = -1$, the convergence is not deteriorated which confirms the theoretical results obtained in both the *a priori* analysis in [16] and the *a posteriori* analysis
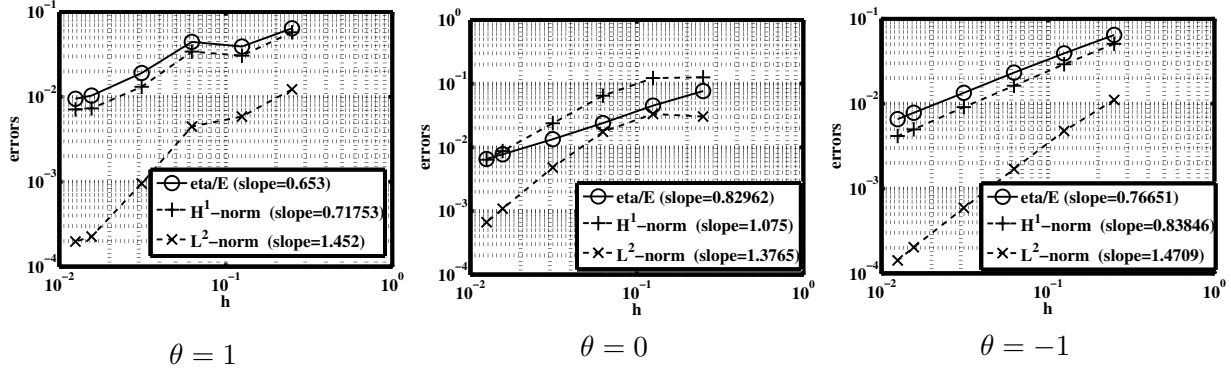
in Section 3 (see Theorem 3.5).

Figure 5: First example. Convergence curves of the error estimator η, the L^2 and H^1-norms of the error $\mathbf{u} - \mathbf{u}^h$, for $\gamma_0 = 1000/E$.

4.1.3 The case of a very large γ_0

Additionally we present a numerical convergence study for $\theta = 1, 0, -1$ and for a very large value of the parameter $\gamma_0 = 10^6/E$, far from its reference value of $1/E$. In this case for $\theta = 1$ and $\theta = 0$ there is no more guarantee of well-posedness and optimal convergence (see [16]). The error estimator η, the L^2 and H^1-norms of the error $\mathbf{u} - \mathbf{u}^h$ are plotted in Figure 6, while Tables 4, 5 and 6 present the different contributions of η.
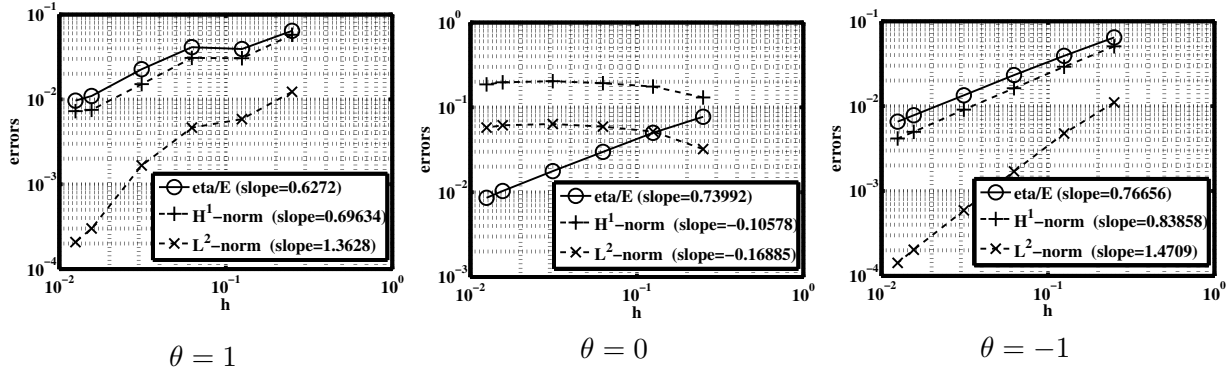

Figure 6: First example. Convergence curves of the error estimator η, the L^2 and H^1-norms of the error $\mathbf{u} - \mathbf{u}^h$, for $\gamma_0 = 10^6/E$.

For the method $\theta = 0$ the solution does not converge while the effectivity index Eff_E tends to 0. This is consistent with our theoretical results since Theorem 3.5 is no more applicable and no upper bound is guaranteed. The estimator η converges despite of the term η_4, slightly increasing but still very small. For the method $\theta = 1$, even though γ_0 is large, the method converges in L^2 and H^1-norms of the error with an acceptable effectivity index, however with a deteriorated convergence rate. Conversely, for the method $\theta = -1$, both convergence and effectivity index are optimal and are not deteriorated compared to the case $\gamma_0 = 1/E$. This supports its theoretical property of robustness with respect to γ_0.

16

Table 4: First example, $\theta = 1$ and $\gamma_0 = 10^6/E$.

Mesh size h	1/4	1/8	1/16	1/32	1/64	1/80	slope
Degrees of freedom	32	128	512	2048	8192	12800	
$\left\|\mathbf{u}-\mathbf{u}^h\right\|_{0,\Omega}$ $(\times 10^{-4})$	122.6500	58.4959	46.4511	16.6143	3.0112	2.0808	1.3628
$\left\|\mathbf{u}-\mathbf{u}^h\right\|_{1,\Omega}$ $(\times 10^{-3})$	57.7770	30.5558	30.8275	15.1381	7.5190	7.2669	0.6963
η_1	16719.8	8359.9	4179.95	2089.97	1044.99	835.99	1.0000
η_2	62073.4	38335.4	41033.3	22552.4	10916.7	9635.48	0.6172
$\eta_3(\times 10^{-2})$	2.13709	1.01961	0.63268	0.768462	0.414401	0.42499	0.4878
$\eta_4(\times 10^{-2})$	2.52415	0.571842	2.55605	1.38494	0.525521	0.446467	0.4177
η	64285.7	39236.3	41245.6	22649	10966.6	9671.68	0.6272
Effectivity index Eff_E	1.1127	1.2841	1.3380	1.4962	1.4564	1.3266	

Table 5: First example, $\theta = 0$ and $\gamma_0 = 10^6/E$.

Mesh size h	1/4	1/8	1/16	1/32	1/64	1/80	slope
Degrees of freedom	32	128	512	2048	8192	12800	
$\left\|\mathbf{u}-\mathbf{u}^h\right\|_{0,\Omega}$ $(\times 10^{-4})$	321.9223	518.2042	592.2560	635.8190	615.1016	577.5225	-0.1689
$\left\|\mathbf{u}-\mathbf{u}^h\right\|_{1,\Omega}$ $(\times 10^{-3})$	130.6775	175.6706	192.4574	203.4624	197.2235	186.4225	-0.1058
η_1	16719.8	8359.9	4179.95	2089.97	1044.99	835.99	1.0000
η_2	75562.4	49342.9	29582.9	17606.7	10284.5	8546.95	0.7339
η_3	2468.7	908.957	316.586	107.411	38.2804	28.2145	1.5045
η_4 $(\times 10^{-1})$	2.00548	3.65123	5.58251	8.52101	1.38006	1.37438	-0.6465
η	77429.5	50054.3	29878.5	17730.7	10337.5	8587.78	0.7399
Effectivity index Eff_E $(\times 10^{-1})$	5.9252	2.8493	1.5525	0.8714	0.5242	0.4607	

Table 6: First example, $\theta = -1$ and $\gamma_0 = 10^6/E$.

Mesh size h	1/4	1/8	1/16	1/32	1/64	1/80	slope
Degrees of freedom	32	128	512	2048	8192	12800	
$\left\|\mathbf{u}-\mathbf{u}^h\right\|_{0,\Omega}$ $(\times 10^{-4})$	110.5852	47.6266	16.9809	5.9093	2.0290	1.4216	1.4709
$\left\|\mathbf{u}-\mathbf{u}^h\right\|_{1,\Omega}$ $(\times 10^{-3})$	50.6403	29.1195	16.2386	9.0861	4.9803	4.1565	0.8386
η_1	16719.8	8359.9	4179.95	2089.97	1044.99	835.99	1.0000
η_2	62292.2	38204	22809.5	13249.4	7732.01	6512.98	0.7582
$\eta_3(\times 10^{-4})$	143.671	83.7405	26.7592	8.72031	3.05775	0.0236947	1.4405
η_4 $(\times 10^{-4})$	168.808	67.5774	14.2866	3.96942	1.17445	0.948677	1.8030
η	64497	39108	23189.4	13413.2	7802.31	6566.42	0.7666
Effectivity index Eff_E	1.2736	1.3430	1.4280	1.4762	1.5663	1.5796	

The previous experiment for $\theta = 0$ reveals the bad behavior of η for a very large γ_0. An heuristics to recover a meaningful estimator is to decouple the value of γ_0 for the problem (5) and for the estimator η_4. A last experiment shows in Figure 7 the convergence curves in the same

case $\gamma_0 = 10^6/E$ yet with an error estimator that makes use of a Nitsche's parameter $\tilde{\gamma}_0 = 1/E$. For the methods $\theta = 1$ and $\theta = -1$ this has no visible influence on the effectivity index Eff_E. For the method $\theta = 0$, a better effectivity index is obtained: at least the estimator does not tend to zero for a non-convergent solution, in contrast with what happens in Figure 6. To summarize, this study for a large γ_0 confirms the analysis provided in Section 3 which requires a sufficiently small parameter γ_0 to obtain a reliable and efficient *a posteriori* estimator when $\theta \neq -1$.
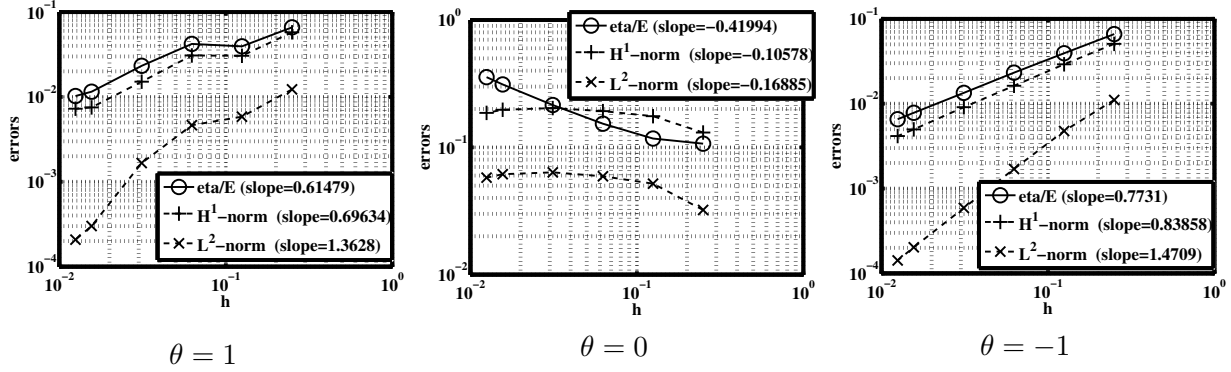

Figure 7: First example. Convergence curves of the error estimator η, the L^2 and H^1-norms of the error $\mathbf{u} - \mathbf{u}^h$, with $\gamma_0 = 10^6/E$ in the Nitsche's method and $\tilde{\gamma}_0 = 1/E$ in the error estimator η_4.

4.2 Second example: Hertz's contact

4.2.1 Description

We consider Hertz's contact problems of a disk/a sphere with a plane rigid foundation (see, e.g., the numerical examples in [16, 31]). The parameters have been fixed as $\theta = -1$ and $\gamma_0 = 10^{-3}/E$.

The disc (resp. the sphere) is of center $(0, 20)$ (resp. of center $(0, 0, 20)$) and radius 20. The lower part of the boundary Γ_C is potentially in contact with the rigid support ; the remaining (upper part) of the boundary Γ_N is subjected to a homogenous Neumann condition. To overcome the non-definiteness coming from free rigid motions, the horizontal displacement is prescribed to be zero on the two points of coordinates $(0, 20)$ and $(0, 25)$ (resp. the horizontal displacement components u_1 and u_2 on the point $(0,0,20)$, the component u_1 on the point $(0,5,20)$ and the component u_2 on the point $(5,0,20)$): this blocks the horizontal translation and the rigid rotation. Young's modulus is fixed at $E = 25$ and Poisson's ratio is $\nu_P = 0.25$. A vertical density of volume forces of intensity 20 is applied in Ω. The reference solutions are depicted in Figure 8. There are refined solutions with an average mesh size $h = 0.10$ for the disc (resp. $h = 1.27$ for the sphere), Lagrange P_2 elements, $\theta = -1$ and $\gamma = 10^{-3}/E$.

The initial gap between Γ_C and the obstacle is computed as $gap(\mathbf{x}) := \mathbf{x} \cdot \mathbf{n}_{\text{obs}}$, where $\mathbf{x} \in \Gamma_C$ and with $\mathbf{n}_{\text{obs}}$ the unit outward normal vector on the boundary of the plane obstacle. The error estimator associated to the contact condition on Γ_C is then slightly modified:

$$\eta_{4K} = h_K^{1/2} \left(\sum_{E \in E_K^C} \left\| \frac{1}{\gamma}[P_\gamma(\mathbf{u}^h) - gap]_+ + \sigma_n(\mathbf{u}^h) \right\|_{0,E}^2 \right)^{1/2}.$$
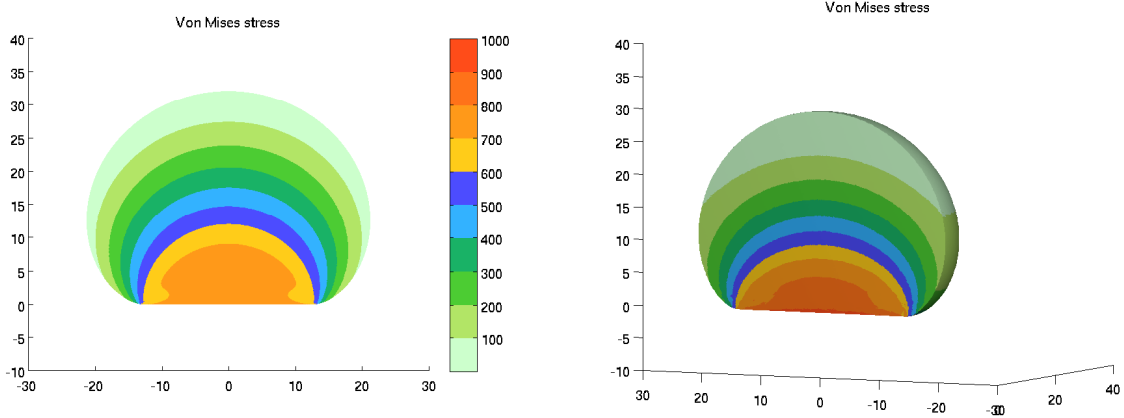
18

Figure 8: Reference solutions with von Mises stresses, in 2D (left) and 3D (right).

4.2.2 Numerical convergence in 2D

The error curves in the 2D case are depicted in Figure 9, both for linear and quadratic finite elements. In the case of P_1 finite elements, and as in [16], a slight super-convergence is observed in the H^1-norm of the error (1.5 instead of 1). This behavior is not recovered by the error estimator η, that converges with a rate close to 1. The origin of this difference is unknown. For P_2 finite elements the agreement between η and the error in H^1-norm is better: for the H^1-norm, the convergence rate is close to 1.7, while of approximately 1.5 for η. We observe the same results for the variants $\theta = 0, 1$.
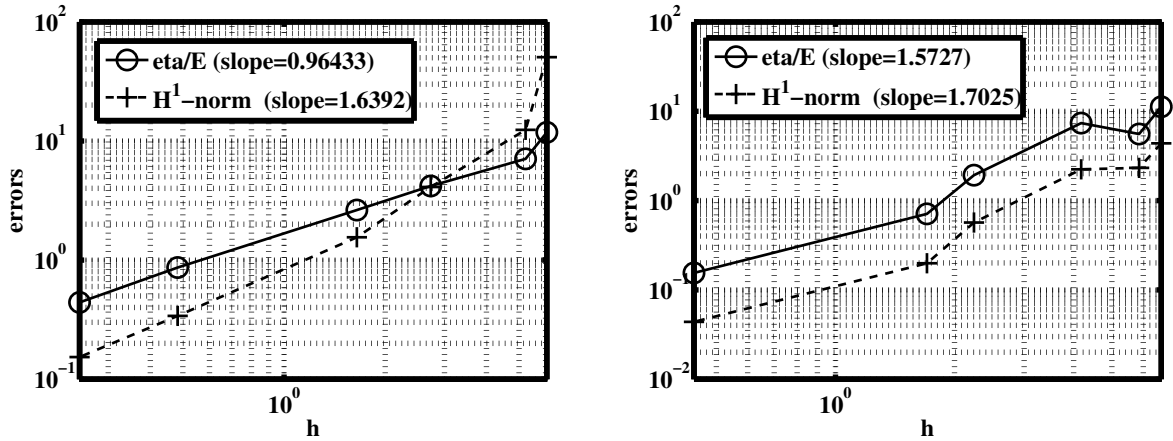

Figure 9: Hertz's contact in 2D. Error estimator η and the H^1-norm of the error $\mathbf{u} - \mathbf{u}^h$, for Lagrange P_1 (left) and P_2 (right) finite elements.

In Table 7 the contribution of each component η_i of η is detailed. Each term of the error estimator converges towards zero when h becomes smaller. Note however the increasing values of the effectivity index, due to the super-convergence in H^1-norm and the convergence rate of the contribution η_4, that is close to 1.5.

Table 7: Hertz's contact in 2D, $\theta = -1$, $\gamma_0 = 10^{-3}/E$ and Lagrange P_1 elements

Mesh size h	6.04766	5.23002	2.7327	1.64637	0.482414	0.246359	slope
$\|\mathbf{u} - \mathbf{u}^h\|_{1,\Omega}$	50.5984	12.3996	4.1083	1.5561	0.3399	0.1534	1.6392
η_1	7781.84	7376.92	4066.11	2379.44	728.236	359.817	0.9715
η_2	18000.7	12350.7	9279.79	5866.83	2009.88	1029.86	0.8525
η_3	2523.15	1055.64	852.542	458.121	90.2956	38.1934	1.2132
η_4	21999.5	10276.6	2537.53	1735.77	321.871	152.501	1.4597
η	29579.2	17711.1	10479.2	6580.59	2163.73	1102.18	0.9643
Effectivity index Eff_E	0.2338	0.5713	1.0203	1.6916	2.5467	2.8735	

4.2.3 Numerical convergence in 3D

The error curves in the 3D case are depicted in Figure 10, both for linear and quadratic finite elements. For P_1 finite elements the convergence rates for η and for the error in H^1-norm are close (around 1.3) and slightly above the expected rate of 1. For P_2 finite elements we observe a sub-optimality of the error estimator η, which converges but with a rate of 1, while the error in H^1-norm remains optimal, with a convergence rate around 1.5.
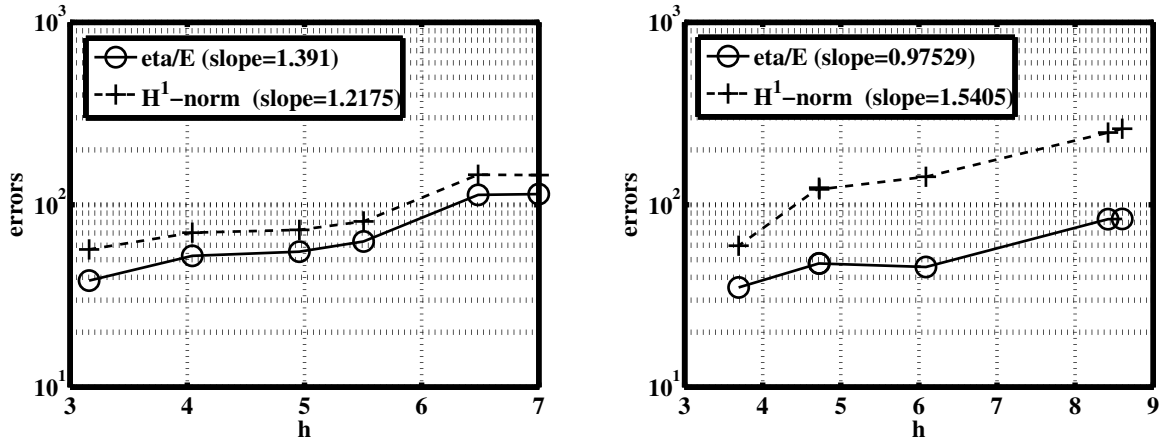

Figure 10: Hertz's contact in 3D. Error estimator η and H^1-norm of the error $\mathbf{u} - \mathbf{u}^h$, for Lagrange P_1 (left) and P_2 (right) finite elements.

Acknowledgements

Appendix 1. Extension to the Tresca friction case

We extend in this appendix the analysis of Section 3 to the case of unilateral contact with Tresca friction. About *a posteriori* error estimates for the Tresca friction problem one may refer, e.g., to

[20] and references therein.

Setting and Nitsche-based finite element method for Tresca

Let $g \in L^2(\Gamma_C)$, $g \geq 0$ be a given threshold. The Tresca friction problem with unilateral contact consists in finding the displacement field $\mathbf{u} : \Omega \to \mathbb{R}^d$ verifying the equations and conditions (1)–(2 (i,ii,iii))–(21), with (21) given by:

$$
\begin{cases}
|\boldsymbol{\sigma}_{\mathbf{t}}(\mathbf{u})| \leq g, & \text{if } \mathbf{u}_{\mathbf{t}} = \mathbf{0}, \quad (i) \\
\boldsymbol{\sigma}_{\mathbf{t}}(\mathbf{u}) = -g\dfrac{\mathbf{u}_{\mathbf{t}}}{|\mathbf{u}_{\mathbf{t}}|} & \text{otherwise}, \quad (ii)
\end{cases}
\tag{21}
$$

where $|\cdot|$ stands for the euclidean norm in $\mathbb{R}^{d-1}$.

For any $\alpha \in \mathbb{R}^+$, we introduce the notation $[\cdot]_\alpha$ for the orthogonal projection onto $\mathscr{B}(\mathbf{0}, \alpha) \subset \mathbb{R}^{d-1}$, where $\mathscr{B}(\mathbf{0}, \alpha)$ is the closed ball centered at the origin $\mathbf{0}$ and of radius α. The following property holds for all $\mathbf{x}, \mathbf{y} \in \mathbb{R}^{d-1}$:

$$
(\mathbf{y} - \mathbf{x}) \cdot ([\mathbf{y}]_\alpha - [\mathbf{x}]_\alpha) \geq |[\mathbf{y}]_\alpha - [\mathbf{x}]_\alpha|^2,
\tag{22}
$$

where $\cdot$ is the euclidean scalar product in $\mathbb{R}^{d-1}$.

Let us introduce the discrete linear operator $\mathbf{P}_\gamma^{\mathbf{t}} : \mathbf{v}^h \mapsto \mathbf{v}_{\mathbf{t}}^h - \gamma\,\boldsymbol{\sigma}_{\mathbf{t}}(\mathbf{v}^h)$ and the bilinear form: $A_{\theta\gamma}(\mathbf{u}^h, \mathbf{v}^h) := a(\mathbf{u}^h, \mathbf{v}^h) - \int_{\Gamma_C} \theta\gamma\,\boldsymbol{\sigma}(\mathbf{u}^h)\mathbf{n} \cdot \boldsymbol{\sigma}(\mathbf{v}^h)\mathbf{n}\, d\Gamma$. The extension of our Nitsche-based method for unilateral contact with Tresca friction then reads:

$$
\begin{cases}
\text{Find } \mathbf{u}^h \in \mathbf{V}^h \text{ such that:} \\
A_{\theta\gamma}(\mathbf{u}^h, \mathbf{v}^h) + \displaystyle\int_{\Gamma_C} \frac{1}{\gamma}\,[P_\gamma(\mathbf{u}^h)]_+ P_{\theta\gamma}(\mathbf{v}^h)\, d\Gamma + \int_{\Gamma_C} \frac{1}{\gamma}\left[\mathbf{P}_\gamma^{\mathbf{t}}(\mathbf{u}^h)\right]_{\gamma g} \cdot \mathbf{P}_{\theta\gamma}^{\mathbf{t}}(\mathbf{v}^h)\, d\Gamma = L(\mathbf{v}^h), \\
\hspace{10cm} \forall\, \mathbf{v}^h \in \mathbf{V}^h.
\end{cases}
\tag{23}
$$

Consistency, well-posedness and *a priori* error estimates for the method (23) are established in [14].

Residual error estimator, upper and lower bound

The Definition 3.2 still holds for problem (23), except for η_{3K} whose expression is now:

$$
\eta_{3K} = h_K^{1/2}\left(\sum_{E \in E_K^C} \left\|\frac{1}{\gamma}\left[\mathbf{P}_\gamma^{\mathbf{t}}(\mathbf{u}^h)\right]_{\gamma g} + \boldsymbol{\sigma}_{\mathbf{t}}(\mathbf{u}^h)\right\|_{0,E}^2\right)^{1/2}.
$$

First we provide counterparts of the Assumption 3.3 and of the discrete trace inequality of Lemma 2.3.

Assumption 4.2. *The solution $\mathbf{u}$ of (1)–(2 (i,ii,iii))–(21) and the discrete solution $\mathbf{u}^h$ of (23) are such that:*

$$
\left\|\sigma_n(\mathbf{u} - \mathbf{u}^h)\right\|_{-1/2,h,\Gamma_C} + \left\|\boldsymbol{\sigma}_{\mathbf{t}}(\mathbf{u} - \mathbf{u}^h)\right\|_{-1/2,h,\Gamma_C} \lesssim \|\mathbf{u} - \mathbf{u}^h\|_{1,\Omega}.
\tag{24}
$$

Lemma 4.3. *For any* $\mathbf{v}^h \in \mathbf{V}^h$, *we have*

$$\|\sigma_n(\mathbf{v}^h)\|_{-1/2,h,\Gamma_C} + \|\boldsymbol{\sigma}_{\mathbf{t}}(\mathbf{v}^h)\|_{-1/2,h,\Gamma_C} \lesssim \|\mathbf{v}^h\|_{1,\Omega}. \tag{25}$$

For contact with Tresca friction, the following statement guarantees the reliability of the *a posteriori* error estimator:

Theorem 4.4. *Let* $\mathbf{u}$ *be the solution to (1)–(2 (i,ii,iii))–(21), with* $\mathbf{u} \in (H^{\frac{3}{2}+\nu}(\Omega))^d$ *($\nu > 0$ and $d = 2, 3$), and let* $\mathbf{u}^h$ *be the solution to the corresponding discrete problem (23). Assume that, for* $\theta \neq -1$, γ_0 *is sufficiently small, and otherwise that* $\gamma_0 > 0$ *for* $\theta = -1$. *Assume that the saturation assumption (24) holds as well. Then we have*

$$\|\mathbf{u} - \mathbf{u}^h\|_{1,\Omega} + \left\| \sigma_n(\mathbf{u}) + \frac{1}{\gamma}[P_\gamma(\mathbf{u}^h)]_+ \right\|_{-1/2,h,\Gamma_C} + \left\| \boldsymbol{\sigma}_{\mathbf{t}}(\mathbf{u}) + \frac{1}{\gamma}\left[\mathbf{P}^{\mathbf{t}}_\gamma(\mathbf{u}^h)\right]_{\gamma g} \right\|_{-1/2,h,\Gamma_C}$$
$$+ \|\sigma_n(\mathbf{u}) - \sigma_n(\mathbf{u}^h)\|_{-1/2,h,\Gamma_C} + \|\boldsymbol{\sigma}_{\mathbf{t}}(\mathbf{u}) - \boldsymbol{\sigma}_{\mathbf{t}}(\mathbf{u}^h)\|_{-1/2,h,\Gamma_C} \lesssim (1 + \gamma_0)\eta + \zeta.$$

Proof: The proof is a direct adaptation of Theorem 3.5. Let $\mathbf{v}^h \in \mathbf{V}^h$. To lighten the notation, we denote $\mathbf{e} := \mathbf{u} - \mathbf{u}^h$. We start as in Theorem 3.5 and get

$$\alpha\|\mathbf{e}\|^2_{1,\Omega} \leq \mathcal{T}_1 + \mathcal{T}_2$$

where α is the $\mathbf{V}$−ellipticity constant of $a(\cdot, \cdot)$ and

$$\mathcal{T}_1 := L(\mathbf{u} - \mathbf{v}^h) - a(\mathbf{u}^h, \mathbf{u} - \mathbf{v}^h) + \int_{\Gamma_C} \frac{1}{\gamma}[P_\gamma(\mathbf{u}^h)]_+(v^h_n - u_n)\,d\Gamma + \int_{\Gamma_C} \frac{1}{\gamma}\left[\mathbf{P}^{\mathbf{t}}_\gamma(\mathbf{u}^h)\right]_{\gamma g} \cdot (\mathbf{v}^h_{\mathbf{t}} - \mathbf{u}_{\mathbf{t}})\,d\Gamma$$

$$\mathcal{T}_2 := \int_{\Gamma_C} \boldsymbol{\sigma}(\mathbf{u})\mathbf{n} \cdot (\mathbf{u} - \mathbf{u}^h)\,d\Gamma + \int_{\Gamma_C} \frac{1}{\gamma}[P_\gamma(\mathbf{u}^h)]_+ P_{\theta\gamma}(\mathbf{u} - \mathbf{u}^h)\,d\Gamma + \int_{\Gamma_C} \frac{1}{\gamma}\left[\mathbf{P}^{\mathbf{t}}_\gamma(\mathbf{u}^h)\right]_{\gamma g} \cdot \mathbf{P}^{\mathbf{t}}_{\theta\gamma}(\mathbf{u} - \mathbf{u}^h)\,d\Gamma$$

$$- \theta\int_{\Gamma_C} \frac{1}{\gamma}[P_\gamma(\mathbf{u}^h)]_+ \gamma\sigma_n(\mathbf{v}^h - \mathbf{u})\,d\Gamma - \theta\int_{\Gamma_C} \frac{1}{\gamma}\left[\mathbf{P}^{\mathbf{t}}_\gamma(\mathbf{u}^h)\right]_{\gamma g} \cdot \gamma\boldsymbol{\sigma}_{\mathbf{t}}(\mathbf{v}^h - \mathbf{u})\,d\Gamma$$

$$- \theta\int_{\Gamma_C} \gamma\,\boldsymbol{\sigma}(\mathbf{u}^h)\mathbf{n} \cdot \boldsymbol{\sigma}(\mathbf{v}^h - \mathbf{u}^h)\mathbf{n}\,d\Gamma.$$

The quantity $\mathcal{T}_1$ is bounded almost exactly as in Theorem 3.5, except for the new Tresca friction term, that is bounded as follows:

$$\left| \sum_{E \in E^C_h} \int_E \left(\frac{1}{\gamma}\left[\mathbf{P}^{\mathbf{t}}_\gamma(\mathbf{u}^h)\right]_{\gamma g} + \boldsymbol{\sigma}_{\mathbf{t}}(\mathbf{u}^h) \right) \cdot (\mathbf{v}^h_{\mathbf{t}} - \mathbf{u}_{\mathbf{t}})\,d\Gamma \right| \lesssim \eta\|\mathbf{e}\|_{1,\Omega}.$$

Note that the remaining terms in $\mathcal{T}_2$ can be split as

$$\mathcal{T}_2 = \mathcal{T}_2^C + \mathcal{T}_2^T,$$

where $\mathcal{T}_2^C$ represents the contact terms and $\mathcal{T}_2^T$ contains the Tresca friction terms. The contact terms $\mathcal{T}_2^C$ are handled as in Theorem 3.5. Moreover, we can bound the friction terms $\mathcal{T}_2^T$ in a similar fashion, following step by step the proof of Theorem 3.5 and using the bound (22). We get finally for any $\beta > 0$:

$$\mathcal{T}_2^T \leq \left(\frac{1}{2\beta} + \frac{(\theta+1)^2}{4} \right) \gamma_0\|\boldsymbol{\sigma}_{\mathbf{t}}(\mathbf{u} - \mathbf{u}^h)\|^2_{-1/2,h,\Gamma_C} + \beta\gamma_0\theta^2\eta^2 + \frac{\gamma_0}{2\beta}\|\boldsymbol{\sigma}_{\mathbf{t}}(\mathbf{v}^h - \mathbf{u}^h)\|^2_{-1/2,h,\Gamma_C}.$$

22

Using (25) and the H^1-stability of R^h (see (8) in Lemma 2.1) we bound:

$$\|\boldsymbol{\sigma_t}(\mathbf{v}^h - \mathbf{u}^h)\|_{-1/2,h,\Gamma_C} \leq C\|\mathbf{v}^h - \mathbf{u}^h\|_{1,\Omega} = C\|R^h(\mathbf{u} - \mathbf{u}^h)\|_{1,\Omega} \leq C\|\mathbf{u} - \mathbf{u}^h\|_{1,\Omega}.$$

We combine this last bound with the saturation assumption (24) and get (remembering that the same result holds for the contact terms $\mathcal{T}_2^C$):

$$\mathcal{T}_2 \leq C\gamma_0 \left(\frac{(\theta + 1)^2}{4} + \frac{1}{\beta} \right) \|\mathbf{u} - \mathbf{u}^h\|_{1,\Omega}^2 + \beta\gamma_0\theta^2\eta^2.$$

From now on the proof is exactly the same as in Theorem 3.5. $\qquad\square$

Remark 4.5. *An extension of Theorem 3.6 holds as well for Problem* (23) *and similar local lower error bounds can be derived following the same method. The only difference is that the term η_{3K} is bounded as follows:*

$$\eta_{3K} \lesssim \sum_{E \in E_K^C} h_K^{1/2} \left(\left\| \boldsymbol{\sigma_t}(\mathbf{u}) + \frac{1}{\gamma} \left[\mathbf{P}_\gamma^{\mathbf{t}}(\mathbf{u}^h) \right]_{\gamma g} \right\|_{0,E} + \left\| \boldsymbol{\sigma_t}(\mathbf{u} - \mathbf{u}^h) \right\|_{0,E} \right).$$

References

[1] R. A. ADAMS, *Sobolev spaces*, Academic Press, New York-London, 1975. Pure and Applied Mathematics, Vol. 65.

[2] M. AINSWORTH AND J. T. ODEN, *A posteriori error estimation in finite element analysis*, Wiley-Interscience, New York, 2000.

[3] P. ALART AND A. CURNIER, *A generalized Newton method for contact problems with friction*, J. Mech. Theor. Appl., 7 (1988), pp. 67–82.

[4] R. BECKER, *Mesh adaptation for Dirichlet flow control via Nitsche's method*, Comm. Numer. Methods Engrg., 18 (2002), pp. 669–680.

[5] R. BECKER, P. HANSBO, AND R. STENBERG, *A finite element method for domain decomposition with non-matching grids*, M2AN Math. Model. Numer. Anal., 37 (2003), pp. 209–225.

[6] R. BECKER AND R. RANNACHER, *A feed-back approach to error control in finite element methods: basic analysis and examples*, East-West J. Numer. Math., 4 (1996), pp. 237–264.

[7] R. BECKER AND R. RANNACHER, *An optimal control approach to a posteriori error estimation in finite element methods*, Acta Numerica, 10 (2001), pp. 1–102.

[8] C. BERNARDI AND V. GIRAULT, *A local regularization operator for triangular and quadrilateral finite elements*, SIAM J. Numer. Anal., 35 (1998), pp. 1893–1916.

[9] H. BLUM AND F. SUTTMEIER, *An adaptive finite element discretization for a simplified Signorini problem*, Calcolo, 37 (2000), pp. 65–77.

[10] D. BRAESS AND R. VERFÜRTH, *A posteriori error estimators for the Raviart-Thomas element*, SIAM J. Numer. Anal., 33 (1996), pp. 2431–2444.

[11] S.-C. Brenner and L.-R. Scott, *The Mathematical Theory of Finite Element Methods*, vol. 15 of Texts in Applied Mathematics, Springer-Verlag, New York, 2007.

[12] C. Carstensen, *A posteriori error estimate for the mixed finite element method*, Math. Comp., 66 (1997), pp. 465–476.

[13] C. Carstensen, O. Scherf, and P. Wriggers, *Adaptive finite elements for elastic bodies in contact*, SIAM J. Sci. Comput., 20 (1999).

[14] F. Chouly, *An adaptation of Nitsche's method to the Tresca friction problem*, J. Math. Anal. Appl., 411 (2014), pp. 329–339.

[15] F. Chouly and P. Hild, *A Nitsche-based method for unilateral contact problems: numerical analysis*, SIAM J. Numer. Anal., 51 (2013), pp. 1295–1307.

[16] F. Chouly, P. Hild, and Y. Renard, *Symmetric and non-symmetric variants of Nitsche's method for contact problems in elasticity: theory and numerical experiments*, Math. Comp, 84 (2015), pp. 1089–1112.

[17] P. G. Ciarlet, *Handbook of Numerical Analysis (eds. P.G. Ciarlet and J.L. Lions)*, vol. II, North Holland, 1991, ch. 1. "The finite element method for elliptic problems", pp. 17–352.

[18] P. Coorevits, P. Hild, and M. Hjiaj, *A posteriori error control of finite element approximations for Coulomb's frictional contact*, SIAM J. Sci. Comput., 23 (2001), pp. 976–999.

[19] P. Coorevits, P. Hild, and J.-P. Pelle, *A posteriori error estimation for unilateral contact with matching and nonmatching meshes*, Comput. Methods Appl. Mech. Engrg., 186 (2000), pp. 65–83.

[20] P. Dörsek and J. M. Melenk, *Adaptive hp-FEM for the contact problem with Tresca friction in linear elasticity: The primal–dual formulation and a posteriori error estimation*, Appl. Numer. Math., 60 (2010), pp. 689–704.

[21] C. Eck and W. Wendland, *A residual-based error estimator for BEM-discretizations of contact problems*, Numer. Math., 95 (2003), pp. 253–282.

[22] A. Ern and J.-L. Guermond, *Theory and practice of finite elements*, vol. 159 of Applied Mathematical Sciences, Springer-Verlag, New York, 2004.

[23] M. Fabre, J. Pousin, and Y. Renard, *A fictitious domain method for frictionless contact problems in elasticity using Nitsche's method*. Submitted. Available on HAL as hal-00960996.

[24] J. R. Fernández and P. Hild, *A posteriori error analysis for the normal compliance problem*, Appl. Numer. Math., 60 (2010), pp. 64–73.

[25] G. Fichera, *Problemi elastostatici con vincoli unilaterali: Il problema di Signorini con ambigue condizioni al contorno*, Atti Accad. Naz. Lincei Mem. Cl. Sci. Fis. Mat. Natur. Sez. I (8), 7 (1963/1964), pp. 91–140.

[26] A. Hansbo and P. Hansbo, *An unfitted finite element method, based on Nitsche's method, for elliptic interface problems*, Comput. Methods Appl. Mech. Engrg., 191 (2002), pp. 5537–5552.

[27] A. HANSBO, P. HANSBO, AND M. G. LARSON, *A finite element method on composite grids based on Nitsche's method*, M2AN Math. Model. Numer. Anal., 37 (2003), pp. 495–514.

[28] J. HASLINGER, I. HLAVÁČEK, AND J. NEČAS, *Handbook of Numerical Analysis (eds. P.G. Ciarlet and J.L. Lions)*, vol. IV, North Holland, 1996, ch. 2. "Numerical methods for unilateral problems in solid mechanics", pp. 313–385.

[29] P. HILD AND V. LLERAS, *Residual error estimators for Coulomb friction*, SIAM J. Numer. Anal., 47 (2009), pp. 3550–3583.

[30] P. HILD AND S. NICAISE, *A posteriori error estimations of residual type for Signorini's problem.*, Numer. Math., 101 (2005), pp. 523–549.

[31] ——, *Residual a posteriori error estimators for contact problems in elasticity*, ESAIM: Mathematical Modelling and Numerical Analysis, 41 (2007), pp. 897–923.

[32] M. JUNTUNEN AND R. STENBERG, *On a mixed discontinuous Galerkin method*, Electron. Trans. Numer. Anal., 32 (2008), pp. 17–32.

[33] ——, *Nitsche's method for general boundary conditions*, Math. Comp., 78 (2009), pp. 1353–1374.

[34] ——, *Analysis of finite element methods for the Brinkman problem*, Calcolo, 47 (2010), pp. 129–147.

[35] N. KIKUCHI AND J. T. ODEN, *Contact problems in elasticity: a study of variational inequalities and finite element methods*, vol. 8 of SIAM Studies in Applied Mathematics, Society for Industrial and Applied Mathematics (SIAM), Philadelphia, PA, 1988.

[36] K. Y. KIM, *A posteriori error analysis for locally conservative mixed methods*, Math. Comp., 76 (2007), pp. 43–66.

[37] J. KÖNNÖ AND R. STENBERG, $H(\mathrm{div})$-*conforming finite elements for the Brinkman problem*, Math. Models Methods Appl. Sci., 21 (2011), pp. 2227–2248.

[38] R. KRAUSE, A. VEESER, AND M. WALLOTH, *An efficient and reliable residual-type a posteriori error estimator for the Signorini problem*, Numer. Math., 130 (2015), pp. 151–197.

[39] T. A. LAURSEN, *Computational contact and impact mechanics*, Springer-Verlag, Berlin, 2003.

[40] C.-Y. LEE AND J.-T. ODEN, *A posteriori error estimation of h-p finite element approximations of frictional contact problems*, Comput. Methods Appl. Mech. Engrg., 113 (1994), pp. 11–45.

[41] V. LLERAS, *Modélisation, analyse et simulation de problèmes de contact en mécanique des solides et des fluides*, PhD thesis, Besançon, 2009.

[42] F. LOUF, J.-P. COMBE, AND J.-P. PELLE, *Constitutive error estimator for the control of contact problems involving friction*, Comput. Struct., 81 (2003), pp. 1759–1772.

[43] M. MAISCHAK AND E. STEPHAN, *Adaptive hp-versions of BEM for Signorini problems*, Appl. Numer. Math., 54 (2005), pp. 425–449.

[44] Y. Renard, *Generalized Newton's methods for the approximation and resolution of frictional contact problems in elasticity*, Comp. Methods Appl. Mech. Engrg., 256 (2013), pp. 38–55.

[45] A. Schröder, *A posteriori error estimates of higher-order finite elements for frictional contact problems*, Comput. Methods Appl. Mech. Engrg., 249–252 (2012).

[46] A. Schröder and A. Rademacher, *Goal-oriented error control in adaptive mixed FEM for Signorini's problem*, Comp. Methods Appl. Mech. Engrg., 200 (2011), pp. 345–355.

[47] R. Verfürth, *A review of a posteriori error estimation techniques for elasticity problems*, Comput. Methods Appl. Mech. Engrg., 176 (1999), pp. 419–440.

[48] A. Weiss and B. I. Wohlmuth, *A posteriori error estimator and error control for contact problems*, Math. Comp., (2009), pp. 1237–1267.

[49] B. I. Wohlmuth, *A residual based error estimator for mortar finite element discretizations*, Numer. Math., 84 (1999), pp. 143–171.

[50] B. I. Wohlmuth, *An a posteriori error estimator for two body contact problems on non-matching meshes*, J. Sci. Comput, 33 (2007), pp. 25–45.

[51] P. Wriggers, *Computational Contact Mechanics (Second Edition)*, Wiley, 2006.

[52] P. Wriggers and O. Scherf, *Different a posteriori error estimators and indicators for contact problems*, Math. Comput. Modelling, 28 (1998).